

RESEARCH ARTICLE | DECEMBER 26 2023

Predicting freezing points of ternary salt solutions with the multisolute osmotic virial equation

Hikmat Binyaminov ; Henry Sun ; Janet A. W. Elliott  



J. Chem. Phys. 159, 244502 (2023)

<https://doi.org/10.1063/5.0169047>

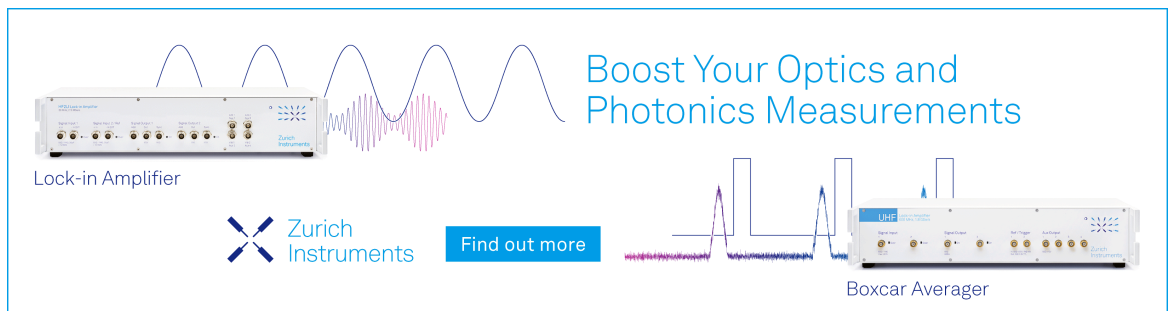


View
Online



Export
Citation

CrossMark



Boost Your Optics and
Photonics Measurements

Lock-in Amplifier

 Zurich
Instruments

[Find out more](#)

Boxcar Averager

Predicting freezing points of ternary salt solutions with the multisolute osmotic virial equation

Cite as: J. Chem. Phys. 159, 244502 (2023); doi: 10.1063/5.0169047

Submitted: 22 July 2023 • Accepted: 5 November 2023 •

Published Online: 26 December 2023



View Online



Export Citation



CrossMark

Hikmat Binyaminov,  Henry Sun,  and Janet A. W. Elliott^{a)} 

AFFILIATIONS

Department of Chemical and Materials Engineering, University of Alberta, Edmonton, Alberta T6G 1H9, Canada

^{a)} Author to whom correspondence should be addressed: janet.elliott@ualberta.ca

ABSTRACT

Previously, the multisolute osmotic virial equation with the combining rules of Elliott *et al.* has been shown to make accurate predictions for multisolute solutions with only single-solute osmotic virial coefficients as inputs. The original combining rules take the form of an arithmetic average for the second-order mixed coefficients and a geometric average for the third-order mixed coefficients. Recently, we derived generalized combining rules from a first principles solution theory, where all mixed coefficients could be expressed as arithmetic averages of suitable binary coefficients. In this work, we empirically extended the new model to account for electrolyte effects, including solute dissociation, and demonstrated its usefulness for calculating the properties of multielectrolyte solutions. First, the osmotic virial coefficients of 31 common salts in water were tabulated based on the available freezing point depression (FPD) data. This was achieved by polynomial fitting, where the degree of the polynomial was determined using a special criterion that accounts for the confidence intervals of the coefficients. Then, the multisolute model was used to predict the FPD of 11 ternary electrolyte solutions. Furthermore, models with the new combining rules and the original combining rules of Elliott *et al.* were compared using both mole fraction and molality as concentration units. We find that the mole-fraction-based model with the new combining rules performs the best and that the results agree well with independent experimental measurements with an all-system root-mean-square error of 0.24 osmoles/kg (0.45 °C) and close to zero mean bias for the entire dataset (371 data points).

Published under an exclusive license by AIP Publishing. <https://doi.org/10.1063/5.0169047>

I. INTRODUCTION

Thermodynamic properties of aqueous salt solutions play a crucial role in many areas of natural, biological, and industrial processes. For example, the characteristics of freezing of the most abundant electrolyte solution on the planet—seawater—are controlled by the salt concentration.¹ Because the concentration and types of the salts in seawater vary, one of the crucial aspects of an accurate ocean model is the reliability of the thermodynamic method used to determine the phase behavior of multicomponent aqueous solutions.^{1,2} In another example, when water vapor condenses on the cloud condensation nuclei in the atmosphere, it dissolves some of the salts from these particles and forms a droplet of an aqueous solution. The path this droplet takes (e.g., whether it evaporates or grows) in the later stages of cloud development is greatly impacted by the types of solutes and their concentrations.^{3,4} Ultimately, the precipitative properties of a cloud are often determined by the microphysical processes that involve aqueous multisolute salt solutions.³ Furthermore,

as aqueous energy storage devices (e.g., aqueous Li-ion, Sn-ion, and Na-ion batteries) evolve and become more practical for commercial use, there is a growing need for a simple and reliable multielectrolyte solution model.^{5–13} One of the main concerns about aqueous batteries is their operability at extreme conditions, such as at temperatures below -20 °C.

There exist many solution theories for nonideal, concentrated multisolute solutions, in-depth discussion of some of which can be found in Refs. 14 and 15. Although maybe accurate, many of these approaches rely on fitting to multisolute solution data, while some require a lot of input model parameters. These characteristics make these models not suitable for general modeling purposes for many engineering applications because of the possibility of many solutes, their different combinations, and a wide range of concentrations. Furthermore, accurate solution theories are usually complicated by nature; hence, their implementation as part of engineering design can be challenging. The desirable qualities of any predictive model are that it should require a minimum number of

fitting parameters, be mathematically simple and computationally cheap, and not rely on multisolute data.

Over the past fifteen years, a form of the osmotic virial equation for multisolute solutions (multisolute osmotic virial equation or MSOVE) has been developed by Elliott *et al.* (the Elliott *et al.* MSOVE or E-MSOVE) that requires only binary solution data (i.e., each solute with the solvent) to predict the chemical potential of a solution with a mixture of solutes.^{16–19} The original single-solute osmotic virial equation is a polynomial equation derived from first principles that expresses osmolality of a single-solute solution as a function of the concentration of the solute.^{20–22} Later, Elliott *et al.*¹⁶ proposed combining rules for osmotic virial coefficients in the regular solution theory framework, which enabled osmotic-virial-equation predictions for multisolute solutions without the need for fitting to multisolute data. By comparing predictions with experimental data, our group has previously demonstrated the accuracy of the molality-based form of the E-MSOVE for solutions of interest in cryobiology, including aqueous mixtures of cryoprotectants and aqueous mixtures of proteins.^{18,23} It was rigorously shown that the molality-based form of the E-MSOVE can be applied to a “grouped solute” representing all solutes when the properties of individual solutes cannot be enumerated,¹⁹ which allows the approach to be applied to complicated intracellular solutions.^{24–27} Additionally, a solute chemical potential equation that is consistent with the molality-based E-MSOVE was derived.^{19,28,29} Furthermore, Prickett *et al.*¹⁷ extended the E-MSOVE to solutions containing electrolytes by introducing an additional single-solute fitting parameter to capture dissociation and other electrolyte effects and showed that this equation could make predictions for aqueous solutions containing NaCl plus another non-electrolyte solute as accurately as if the NaCl contributions had been calculated by the Pitzer–Debye–Hückel model—a more sophisticated electrolyte theory with more fitting parameters. The E-MSOVE was shown to make accurate predictions for many aqueous solutions containing NaCl and one or two other non-electrolyte solutes.^{18,23} Liu *et al.*³⁰ used the mole-fraction-based E-MOSVE to make predictions of the freezing points of multi-electrolyte solutions of interest to zinc–air batteries but without comparison to experimental data. While the previous work suggests that multielectrolyte solution osmolalities could be predicted with the E-MSOVE, this proposition has not been tested.

Recently,³¹ we further explored the theoretical aspects of the MSOVE and developed generalized combining rules for coefficients of arbitrary order in a specific solution theory framework. All newly derived combining rules take the form of an arithmetic-average of suitable pure-term coefficients, which contrasts with the geometric-average combining rule used for the cubic terms in the E-MSOVE implementation. In the previous applications of the E-MSOVE (mainly in cryobiology), most solutions were described sufficiently well by only the first- and second-order terms, and predictions using the geometric-average combining rule for the cubic-order terms were accurate enough for the application. Here, we find that some ternary salt solutions require a third-order combining rule for accurate predictions and that there are enough accurate multielectrolyte solution data to compare different combining rules quantitatively.

The main goal of this article is to demonstrate the viability of the MSOVE with new combining rules (the new MSOVE) for predicting thermodynamic properties of multicomponent salt

solutions. This paper is organized as follows: We start by introducing the necessary formalism, describing the models, and detailing the fitting procedure. Then, we tabulate the mole-fraction- and molality-based osmotic virial coefficients of 31 aqueous binary mixtures of common salts by fitting to binary FPD data taken from the literature. Using the obtained mole-fraction-based binary coefficients in the new MSOVE, we make predictions for 11 ternary combinations (i.e., two salts plus water) of the listed salts for which experimental data are available in the literature for comparison. We conclude by comparing the prediction accuracy of the E-MSOVE and the new MSOVE in molality and mole fraction concentration units.

II. METHODS

A. Virial expansion and the original combining rules

Osmolality is a measure of change in chemical potential of the solvent in the presence of solutes, mathematically defined as¹⁶

$$\pi = -\frac{\mu_1 - \mu_1^\circ}{RTM_1}, \quad (1)$$

where π is the osmolality (with units of osmoles/kg), μ_1 is the chemical potential of the solvent in solution (in this work, the only solvent is water), μ_1° is the chemical potential of the pure solvent, R is the universal gas constant, T is absolute temperature, and M_1 is the molar mass of the solvent. Osmolality can be related to other thermodynamic properties of the solution, such as its FPD and osmotic pressure. Needed for the purposes of the present study, the following expression establishes the relationship between the osmolality and the FPD of a solution:¹⁸

$$\pi = \frac{T_m^\circ - T_m}{RT_m \left(\frac{M_1}{\Delta s_{f,1}^\circ} \right)} = \frac{\Delta T_m \Delta s_{f,1}^\circ}{RM_1 (T_m^\circ - \Delta T_m)}, \quad (2)$$

where ΔT_m represents the FPD, with T_m and T_m° being the freezing point of the solution, and the freezing point of the pure solvent, respectively, and $\Delta s_{f,1}^\circ$ is the standard molar entropy change of fusion of the solvent at the freezing point of the pure solvent. We emphasize that since the reference state in Eq. (2) is pure water, Eq. (2) should only be used for solutions where the concentration of the solute is below the eutectic composition.

The single-solute osmotic virial equation is a polynomial equation for the osmolality of a binary solution expressed in terms of the concentration of the solute.¹⁶ Originally developed in terms of molarity (moles of solute per liter of solution) by McMillan and Mayer²⁰ and later modified to use molality (moles of solute per kilogram of solvent) and mole fraction by Hill,^{21,22} this polynomial expansion can be written as a function in different concentration units with underlying self-consistent solution theories in different sets of independent variables. For a single solute, one form of this expansion in terms of the molality of the solute is given below, which follows the solution theory of Landau and Lifshitz:³²

$$\pi = m_i + B_i m_i^2 + C_i m_i^3 + \dots, \quad (3)$$

where B_i and C_i are the second and the third osmotic virial coefficients of solute i , respectively (conventionally, i starts from $i = 2$, and subscript “1” is used to refer to the solvent). Physically, B_i and C_i correspond to interactions between two and three solute molecules in

the solution, respectively. m_i represents the molality of solute i . This expression was phenomenologically extended by Prickett *et al.*¹⁷ to electrolyte solutions by modifying the osmolality equation as

$$\pi = k_i m_i + B_i (k_i m_i)^2 + C_i (k_i m_i)^3 + \dots, \quad (4)$$

where k_i is a fitting parameter, conventionally referred to as the dissociation constant of electrolyte i , although it empirically accounts for various electrolyte effects (e.g., ionic dissociation, charge screening, etc.) and might not indicate the actual degree of dissociation of the solute when obtained from fitting to data.^{17,33} For non-electrolytes, $k_i = 1$ can be used, recovering the original form of the polynomial. Often, the polynomial can be truncated after the second-order term, or sometimes after the third-order term, while still accurately describing the behavior of the solution. For example, Eq. (4) truncated to the second-order term, with only two fitting parameters (k_i and B_i), can describe the NaCl + H₂O data as accurately as the Pitzer–Debye–Hückel model, which is a sophisticated model requiring six parameters.¹⁷

Suggested by Elliott *et al.*¹⁶ and Prickett *et al.*,¹⁷ combining rules for the osmotic virial coefficients can be used to predict the osmolality of a solution with more than one solute. Truncated to the third-order terms, for $r - 1$ solutes (together with the solvent, there are r components), the molality-based E-MSOVE has the following general form:¹⁶

$$\pi = \sum_{i=2}^r k_i m_i + \sum_{i=2}^r \sum_{j=2}^r B_{ij} k_i m_i k_j m_j + \sum_{i=2}^r \sum_{j=2}^r \sum_{k=2}^r C_{ijk} k_i m_i k_j m_j k_k m_k, \quad (5)$$

for which the following combining rules for the mixed osmotic virial coefficients were proposed:¹⁶

$$B_{ij} = \frac{B_i + B_j}{2} \quad (6)$$

for the second-order term, which accounts for interactions between two solutes i and j , and¹⁶

$$C_{ijk} = (C_i C_j C_k)^{1/3} \quad (7)$$

for the third-order term, which accounts for interactions among the three solutes i , j , and k . The importance of Eq. (5) (together with the combining rules) is that it can be used to predict osmolality of a multisolute solution with parameters obtained from the fits to binary solution data only (i.e., two-component solutions of each solute with the solvent). However, care should be taken when extrapolating Eq. (5) beyond the regression range (i.e., the data range from which the pure coefficients were obtained) because the combining rules given by Eqs. (6) and (7) may not account for various effects, such as the ionic strength dependence in the case of electrolyte solutions.^{17,33}

B. New combining rules for the third and higher-order coefficients

In our recent work,³¹ we theoretically explored a generalized multicomponent solution model and obtained combining rules for any-order coefficients of the mole-fraction-based MSOVE in the form of arithmetic-averages of suitable pure coefficients. That is,

with the mole-fraction-based formulation, we obtained an equivalent of Eq. (6), but the equivalent of the third-order combining rule in Eq. (7) is different; in that, it is also an arithmetic-average of suitable third-order pure coefficients. The new model allows for arbitrary-order polynomials to be combined in a similar fashion, unlike the original combining rules, which are limited to quadratic and cubic polynomials.

In the present work, we find that every binary electrolyte mixture is described well by at most a cubic polynomial. Therefore, we only need the second- and third-order mixed coefficients from the new model, and they take the following forms:

$$B_{ij}^+ = \frac{B_i^+ + B_j^+}{2} \quad (8)$$

and

$$C_{ijk}^+ = \frac{C_i^+ + C_j^+ + C_k^+}{3}, \quad (9)$$

respectively. Since the new model was derived with mole fractions of the solutes as variables, we use the superscript “+” to distinguish the mole-fraction-based coefficients from the molality-based coefficients. The corresponding mole-fraction-based MSOVE, truncated to the third-order terms, takes the following form:

$$\pi^+ = \sum_{i=2}^r k_i^+ x_i + \sum_{i=2}^r \sum_{j=2}^r B_{ij}^+ k_i^+ x_i k_j^+ x_j + \sum_{i=2}^r \sum_{j=2}^r \sum_{k=2}^r C_{ijk}^+ k_i^+ x_i k_j^+ x_j k_k^+ x_k, \quad (10)$$

where x_i is the mole fraction of species i in the solution and $\pi^+ = \pi M_1$ is referred to as the osmole fraction of the solvent.^{18,33} Note that similar to the modification presented in Ref. 17 and used in Eq. (5), we introduce the mole-fraction-based dissociation constants, k_i^+ 's, empirically in Eq. (10) to account for the dissociation of the salts. In our theoretical work,³¹ we only considered nondissociating solutes (i.e., $k_i^+ = 1$ for all i). We will not attempt a justification here; hence, like k_i 's in Eq. (5), k_i^+ 's should be viewed as empirical fitting parameters only.

Equation (10) has been previously used¹⁸ as the mole-fraction-based counterpart of Eq. (5), however, not with the arithmetic-average combining rule for C_{ijk}^+ [i.e., Eq. (9)]. Note that the two models truncated to the third-order terms and written for the same concentration units only differ in the combining rule for the third-order mixed coefficients.

For most calculations in this work, conversion from molality to mole fraction or vice versa is needed. For component i in an aqueous solution, the relationship between the mole fraction and the molality is given as

$$x_i = \frac{M_1 m_i}{1 + M_1 \sum_{i=2}^r m_i}. \quad (11)$$

The numerical values of the constants used for calculations in this work are given in the supplementary material.

Throughout the text, we present the results in osmolality units and refer to osmolalities obtained from the FPD data via Eq. (2) as “experimental data” for brevity. Alternatively, we could invert Eq. (2) and use it to convert osmolality (osmole fraction) calculated from Eq. (5) [Eq. (10)] to FPD and compare the predictions

directly to the true experimental FPD data. Clearly, both methods are equivalent for the purposes of evaluating the models.

C. Determination of the osmotic virial coefficients

As detailed by our group's previous work,¹⁸ (multiple linear) regression through the origin (RTO) is implemented on the binary data in MATLAB (v. 2021a, Natick, MA, USA) to obtain the binary osmotic virial coefficients. The method is essentially polynomial fitting of a chosen degree with a matrix method, where the constant term of the polynomial is set to zero. The general form of the matrix regression model is expressed as

$$y = \mathbf{F}\beta + \varepsilon, \quad (12)$$

where y is the vector of calculated osmolalities (or osmole fractions), \mathbf{F} is the matrix of regressors, and ε is the vector of model prediction errors. β is the vector of regression coefficients, and it is calculated as

$$\beta = (\mathbf{F}^T \mathbf{F})^{-1} \mathbf{F}^T y. \quad (13)$$

The estimated model variance is calculated as

$$\sigma^2 = \frac{\sum_{i=1}^n (y_i - \bar{y}_i)^2}{n - p}, \quad (14)$$

where y_i represents the i th data point, \bar{y}_i is the model prediction at that data point, n is the number of data points used in the fit, and p is the degree of the polynomial.

With the covariance matrix being $\mathbf{S} = (\mathbf{F}^T \mathbf{F})^{-1}$, the 95% confidence intervals (CI) are calculated as

$$\beta_i \pm t_{\frac{\alpha}{2}, n-p} \sqrt{\sigma^2 S_{ii}}, \quad (15)$$

where β_i is the i th element of β and $t_{\frac{\alpha}{2}, n-p}$ is the α th percentile of the Student's t -distribution for $n - p$ degrees of freedom. S_{ii} is the i th diagonal element of the covariance matrix.

As the metric to determine the degree of the polynomial fit, we use the RTO-adjusted-R-squared value, defined as¹⁸

$$R_{RTO,adj}^2 = 1 - \frac{\sum_{i=1}^n (y_i - \bar{y}_i)^2 / (n - p)}{\sum_{i=1}^n (y_i^2 / n)}, \quad (16)$$

combined with the relative width of the 95% CIs of the coefficients as described directly below.

For each given dataset, the $R_{RTO,adj}^2$ and the 95% CIs of the coefficients are linearly combined into a single criterion. The combined criterion is deemed necessary because using only the value of $R_{RTO,adj}^2$ to justify the degree of the polynomial may result in large CIs for some datasets (i.e., overfitting). On the other hand, only using the CIs of the coefficients (i.e., looking for the narrowest CIs) to determine the degree of polynomial is not desirable (i.e., underfitting) because sometimes a much better fit (in terms of $R_{RTO,adj}^2$) can be obtained while still having reasonable CIs. The proposed formula for the combined criterion is expressed as

$$\zeta = 100\eta R_{RTO,adj}^2 + (1 - \eta) \frac{\bar{y}_{\max}}{\bar{y}_{95^+, \max}}, \quad (17)$$

where \bar{y}_{\max} denotes the model prediction at the highest experimental concentration and $\bar{y}_{95^+, \max}$ denotes the model prediction at the highest experimental concentration corresponding to the upper bound of the 95% CIs on the coefficients. As a continuous function of concentration, \bar{y}_{95^+} is constructed by taking all coefficients at the upper bounds of their 95% CIs. Note that this method is different than the typical way of calculating the 95% CI of a fit in statistical analysis, which generally improves (i.e., gets more confident) with increasing the degree of the polynomial and, therefore, is not suitable for our purposes. In Eq. (17), η is an adjustable parameter between zero and one that determines the balance between a purely confidence-based fit ($\eta = 0$) and a purely $R_{RTO,adj}^2$ -based fit ($\eta = 1$). When performing the fits, for each given binary mixture dataset, a series of polynomial models are generated up to $p = 5$ at fixed η , out of which the one with the highest ζ value is picked as the best fit.

The first term on the right-hand side of Eq. (17) is multiplied by 100 to assign appropriate weights to each term. For example, the changes of $\Delta R_{RTO,adj}^2 = 0.001$ and $\Delta \left(\frac{\bar{y}_{\max}}{\bar{y}_{95^+, \max}} \right) = 0.1$ have the same weights for the value of $\eta = 0.5$. In other words, ζ is made 100 times more sensitive to a change in $R_{RTO,adj}^2$ compared to the change in the relative width of the CI, $\frac{\bar{y}_{\max}}{\bar{y}_{95^+, \max}}$. This is because, without scaling, $R_{RTO,adj}^2$ is not particularly sensitive to the goodness of the fit, often changing by less than 1% when increasing the degree of the polynomial. Clearly, other choices can be made regarding the functional form of the combined criterion. The idea is to reward for goodness of the fit (in terms of $R_{RTO,adj}^2$) while penalizing for large CIs of the coefficients.

III. RESULTS

A. Tabulation of osmotic virial coefficients

Most of the binary FPD data were collected from the CRC Handbook of Chemistry and Physics³⁴ (CRC or CRC handbook hereafter). The exceptions are as follows: the binary data for ZnCl_2 and ZnBr_2 (obtained from Haghghi *et al.*³⁵) and MgCl_2 (obtained from Gibbard and Gossmann³⁶) because the CRC does not list these salts. Additionally, we also use the CaCl_2 binary data of Oakes *et al.*³⁷ instead of the CRC data because the Oakes *et al.*³⁷ dataset has significantly more data points (55 vs 27), and the fit confidence is significantly higher (when comparing the same-degree fits). The data in the CRC³⁴ are given as FPD vs molality. The data in Gibbard and Gossmann³⁶ are given as FPD vs equivalent concentration, and the data in Haghghi *et al.*³⁵ are given as FPD vs mass percent of the solutes. All datasets from Gibbard and Gossmann³⁶ and Haghghi *et al.*³⁵ were converted to molality (then to mole fraction, where needed) using suitable equations. These unit-conversion equations are detailed in the supplementary material.

After iteratively adjusting η , we found that $\eta = 0.3$ gives a good balance of accuracy and relatively narrow CIs for coefficients of all binary-mixture polynomials needed in this study. When we made the mole-fraction-based fitting significantly more sensitive to $R_{RTO,adj}^2$ by increasing η from 0.3 up to 0.6, it did not affect the degree of fits of most salts except for ZnBr_2 , ZnCl_2 , $\text{Na}_2\text{S}_2\text{O}_3$, ZnSO_4 , and MgSO_4 . With $\eta = 0.6$: (i) for ZnCl_2 , the fit confidence was unacceptably low due to the lack of number of experimental data points; (ii) for MgSO_4 and ZnBr_2 , the fit confidences were considerably

TABLE I. Mole-fraction-based binary fit coefficients and related data. The coefficients were obtained by fitting to data after converting molality to mole fraction and FPD to osmole fraction. The data used for fitting are mainly from the CRC handbook³⁴ except where indicated by a superscript letter, in which case the data are obtained from the work of (a) Oakes *et al.*,³⁷ (b) Gibbard and Gossmann,³⁶ and (c) Haghighi *et al.*³⁵

| Salt | $k^+ \pm 95\%CI$ | $B^+ \pm 95\%CI$ | $C^+ \pm 95\%CI$ | n | Data limit (mole fraction) | $R^2_{RTO,adj}$ | p |
|---|------------------|-------------------|-------------------|-----|----------------------------|-----------------|-----|
| CaCl ₂ ^a | 3.0464 ± 0.1607 | -0.8134 ± 0.7336 | 51.5453 ± 8.5203 | 55 | 0.0664 | 1.0000 | 3 |
| FeCl ₃ | 3.3444 ± 0.4780 | 1.5734 ± 2.9214 | 79.9373 ± 36.7256 | 19 | 0.0497 | 0.9997 | 3 |
| K ₂ CO ₃ | 2.3384 ± 0.0513 | 0.2501 ± 0.3986 | 35.2213 ± 2.8489 | 21 | 0.08 | 1.0000 | 3 |
| NaCl | 1.8348 ± 0.0048 | 0.2853 ± 0.0533 | 14.8930 ± 0.2823 | 32 | 0.0843 | 1.0000 | 3 |
| MgCl ₂ ^b | 2.5265 ± 0.0389 | 5.2909 ± 0.5892 | 84.8666 ± 6.1064 | 30 | 0.0352 | 1.0000 | 3 |
| LiCl | 1.5655 ± 0.0452 | 11.5691 ± 0.7648 | | 13 | 0.0647 | 0.9999 | 2 |
| KI | 1.7730 ± 0.0078 | 1.5885 ± 0.0495 | | 25 | 0.0675 | 1.0000 | 2 |
| KBr | 1.7547 ± 0.0077 | 1.0952 ± 0.0515 | | 27 | 0.0665 | 1.0000 | 2 |
| ZnBr ₂ ^c | 0.7874 ± 0.0886 | 3.6988 ± 1.1404 | | 5 | 0.2106 | 0.9998 | 2 |
| SrCl ₂ | 2.1184 ± 0.0633 | 14.6683 ± 1.0209 | | 18 | 0.0346 | 0.9999 | 2 |
| NaNO ₃ | 1.6950 ± 0.0220 | -0.9503 ± 0.1334 | | 17 | 0.0761 | 0.9999 | 2 |
| NH ₄ Cl | 1.7336 ± 0.0146 | 1.6858 ± 0.1298 | | 14 | 0.0479 | 1.0000 | 2 |
| ZnCl ₂ ^c | 1.4260 ± 0.2031 | | | 4 | 0.1213 | 0.9920 | 1 |
| NaBr | 1.8654 ± 0.0085 | -0.0311 ± 0.2142 | 30.8505 ± 2.4431 | 18 | 0.0346 | 1.0000 | 3 |
| CsCl | 1.7036 ± 0.0067 | | | 30 | 0.0261 | 0.9999 | 1 |
| KCl | 1.8176 ± 0.0063 | | | 14 | 0.0348 | 1.0000 | 1 |
| Na ₂ S ₂ O ₃ | 1.9556 ± 0.0368 | | | 16 | 0.0277 | 0.9988 | 1 |
| MnSO ₄ | 0.9304 ± 0.0468 | 13.3605 ± 2.7310 | | 20 | 0.0290 | 0.9995 | 2 |
| (NH ₄) ₂ SO ₄ | 2.0757 ± 0.0492 | -2.4553 ± 0.5976 | | 14 | 0.0253 | 0.9998 | 2 |
| BaCl ₂ | 2.3985 ± 0.0378 | 4.7370 ± 0.5468 | | 14 | 0.0162 | 0.9999 | 2 |
| MgSO ₄ | 0.9363 ± 0.0801 | 13.2531 ± 4.8420 | | 14 | 0.0277 | 0.9987 | 2 |
| NaC ₂ H ₃ O ₂ | 1.8381 ± 0.0142 | 3.8493 ± 0.2510 | | 10 | 0.0213 | 1.0000 | 2 |
| AgNO ₃ | 1.7860 ± 0.0115 | -5.9317 ± 0.2486 | | 14 | 0.0198 | 1.0000 | 2 |
| ZnSO ₄ | 1.0390 ± 0.0168 | | | 17 | 0.0208 | 0.9990 | 1 |
| KNO ₃ | 1.7459 ± 0.0241 | -6.1918 ± 0.5320 | | 11 | 0.0194 | 1.0000 | 2 |
| CuSO ₄ | 0.9377 ± 0.0111 | | | 15 | 0.0180 | 0.9995 | 1 |
| Na ₂ CO ₃ | 1.9626 ± 0.0666 | | | 7 | 0.0107 | 0.9987 | 1 |
| Na ₂ SO ₄ | 2.4642 ± 0.0627 | -11.7675 ± 1.6586 | | 7 | 0.0080 | 0.9999 | 2 |
| K ₂ SO ₄ | 2.4229 ± 0.0579 | -10.3976 ± 2.2870 | | 9 | 0.0054 | 0.9999 | 2 |
| Na ₃ PO ₄ | 3.5327 ± 0.1045 | -22.6001 ± 3.7881 | | 5 | 0.0028 | 1.0000 | 2 |
| KMnO ₄ | 1.8128 ± 0.0327 | | | 4 | 0.0023 | 0.9999 | 1 |

lower, although they may be usable in some settings; and (iii) for Na₂S₂O₃ and ZnSO₄, the fit confidences were still high, although the data were sufficiently well described by the lower-degree fits as well. Since none of these salts are used in this study to make predictions, the value of η in a reasonable range does not affect the prediction results, and we decided to pick a more conservative value of $\eta = 0.3$. The only salt for which this value of η results in the fitted polynomial having a different degree for the molality-based fit is ZnBr₂, which changes from being a linear function in the mole-fraction-based case to a quadratic function in the molality-based case.

The resulting mole-fraction-based fit parameters are listed in Table I, and the molality-based fit parameters are listed in Table II, with each table containing additional columns for the number of data points used for the fitting, the data limit for each dataset, the value of $R^2_{RTO,adj}$, and the degree of the polynomial fit. For the method of estimation of uncertainties in the coefficients and the graphical representations of the fits, see the supplementary material.

With $\eta = 0.3$, it is apparent that aqueous solutions of most salts can be accurately modeled with only a linear and a quadratic term with only six binaries requiring a cubic term. Naturally, in all cases, the degree and/or the confidence of the fits can be improved by including more high-quality experimental data points. Additionally, since the fitted polynomials are forced to pass through the origin, they have varying sensitivity to the accuracy of experimental data at different concentrations. Therefore, it is important to have more high-quality data points covering the entire concentration range to obtain smaller CIs.

When it comes to the physical meaning of the coefficients, if we assume that the empirical extension due to the electrolyte effects is correct in its functional form (i.e., the modification by a multiplicative constant from m_i to $k_i m_i$ or from x_i to $k_i^+ x_i$), the B_i 's and C_i 's (or the B_i^+ 's and C_i^+ 's) can be interpreted as the second and third osmotic virial coefficients of the salt (see Ref. 31) with the numerical values of these parameters fitted to experimental data also being

TABLE II. Molality-based binary fit coefficients and related data. The coefficients were obtained by fitting to data after converting all concentration units to molality and FPD to osmolality. The data used for fitting are mainly from the CRC handbook³⁴ except where indicated by a superscript letter, in which case the data are obtained from the work of (a) Oakes *et al.*,³⁷ (b) Gibbard and Gossmann,³⁶ and (c) Haghighi *et al.*³⁵

| Salt | $k \pm 95\%CI$ | $B \pm 95\%CI$ (kg/osmoles) | $C \pm 95\%CI$ (kg ² /osmoles ²) | n | Data limit (molality) | $R^2_{RTO,adj}$ | p |
|---|-----------------|-----------------------------|---|-----|-----------------------|-----------------|-----|
| CaCl ₂ ^a | 2.8116 ± 0.1172 | 0.0209 ± 0.0107 | 0.0142 ± 0.0019 | 55 | 3.9465 | 1.0000 | 3 |
| FeCl ₃ | 3.2165 ± 0.4169 | 0.0568 ± 0.0490 | 0.0218 ± 0.0093 | 19 | 2.9010 | 0.9997 | 3 |
| K ₂ CO ₃ | 2.2362 ± 0.0718 | 0.0236 ± 0.0101 | 0.0079 ± 0.0010 | 21 | 4.8240 | 1.0000 | 3 |
| NaCl | 1.8092 ± 0.0047 | 0.0046 ± 0.0009 | 0.0030 ± 0.0001 | 32 | 5.111 | 1.0000 | 3 |
| MgCl ₂ ^b | 2.5045 ± 0.0354 | 0.1021 ± 0.0096 | 0.0220 ± 0.0016 | 30 | 2.0225 | 1.0000 | 3 |
| LiCl | 1.6571 ± 0.0265 | 0.1454 ± 0.0057 | | 13 | 3.8400 | 1.0000 | 2 |
| KI | 1.7861 ± 0.0059 | 0.0143 ± 0.0006 | | 25 | 4.0160 | 1.0000 | 2 |
| KBr | 1.7620 ± 0.0061 | 0.0071 ± 0.0007 | | 27 | 3.9540 | 1.0000 | 2 |
| ZnBr ₂ ^c | 0.9796 ± 0.0593 | | | 5 | 14.8081 | 0.9976 | 1 |
| SrCl ₂ | 2.1730 ± 0.0472 | 0.2214 ± 0.0116 | | 18 | 1.9920 | 0.9999 | 2 |
| NaNO ₃ | 1.6793 ± 0.0244 | -0.0238 ± 0.0026 | | 17 | 4.5750 | 0.9999 | 2 |
| NH ₄ Cl | 1.7410 ± 0.0119 | 0.0167 ± 0.0018 | | 14 | 2.7930 | 1.0000 | 2 |
| ZnCl ₂ ^c | 1.2791 ± 0.1206 | | | 4 | 7.6619 | 0.9965 | 1 |
| NaBr | 1.8610 ± 0.0079 | -0.0064 ± 0.0035 | 0.0083 ± 0.0007 | 18 | 1.9910 | 1.0000 | 3 |
| CsCl | 1.6714 ± 0.01 | | | 30 | 1.4850 | 0.9997 | 1 |
| KCl | 1.7685 ± 0.0042 | | | 14 | 2.0040 | 1.0000 | 1 |
| Na ₂ S ₂ O ₃ | 1.9150 ± 0.0421 | | | 16 | 1.5810 | 0.9983 | 1 |
| MnSO ₄ | 0.9367 ± 0.0439 | 0.2019 ± 0.0430 | | 20 | 1.6560 | 0.9995 | 2 |
| (NH ₄) ₂ SO ₄ | 2.0690 ± 0.0496 | -0.0498 ± 0.0107 | | 14 | 1.4410 | 0.9998 | 2 |
| BaCl ₂ | 2.4036 ± 0.0367 | 0.0740 ± 0.0093 | | 14 | 0.9150 | 0.9999 | 2 |
| MgSO ₄ | 0.9415 ± 0.0762 | 0.2019 ± 0.0777 | | 14 | 1.5820 | 0.9988 | 2 |
| NaC ₂ H ₃ O ₂ | 1.8427 ± 0.0130 | 0.0556 ± 0.0040 | | 10 | 1.2060 | 1.0000 | 2 |
| AgNO ₃ | 1.7798 ± 0.0125 | -0.1118 ± 0.0048 | | 14 | 1.1210 | 1.0000 | 2 |
| ZnSO ₄ | 1.0225 ± 0.0159 | | | 17 | 1.1800 | 0.9991 | 1 |
| KNO ₃ | 1.7392 ± 0.0256 | -0.1165 ± 0.0101 | | 11 | 1.0990 | 1.0000 | 2 |
| CuSO ₄ | 0.9246 ± 0.0117 | | | 15 | 1.0200 | 0.9995 | 1 |
| Na ₂ CO ₃ | 1.9455 ± 0.0694 | | | 7 | 0.6020 | 0.9985 | 1 |
| Na ₂ SO ₄ | 2.4600 ± 0.0632 | -0.2152 ± 0.0301 | | 7 | 0.4490 | 0.9999 | 2 |
| K ₂ SO ₄ | 2.4210 ± 0.0581 | -0.1920 ± 0.0412 | | 9 | 0.3020 | 0.9999 | 2 |
| Na ₃ PO ₄ | 3.5306 ± 0.1027 | -0.4095 ± 0.0670 | | 5 | 0.1560 | 1.0000 | 2 |
| KMnO ₄ | 1.8092 ± 0.0335 | | | 4 | 0.1280 | 0.9999 | 1 |

affected by the truncation of the polynomial. Although it is understood that the values of the k_i 's (or the k_i^+ 's) reflect the collective effects of solute dissociation (i.e., stoichiometric coefficients of the salt), ion charge, ion size, etc., their interpretation is not straightforward since various electrolyte effects are not explicitly accounted for in the model.

Nevertheless, analyzing the numerical values of the k_i^+ 's in Table I, they show clear dependence on the salt's stoichiometric coefficients and the charge of the ions (the k_i 's in Table II have similar values):

- (1) All 1:1 salts with monovalent ions (NaCl, LiCl, KI, KBr, NaNO₃, NH₄Cl, NaBr, CsCl, KCl, NaC₂H₃O₂, AgNO₃, KNO₃, and KMnO₄) have dissociation constants between 1.5 and 2, whereas for 1:1 salts with bivalent ions (MnSO₄, MgSO₄, ZnSO₄, and CuSO₄), the dissociation constants are close to unity.

- (2) All 2:1 salts with monovalent cations and bivalent anions [K₂CO₃, Na₂S₂O₃, (NH₄)₂SO₄, Na₂CO₃, Na₂SO₄, and K₂SO₄] have dissociation constants between 2 and 2.5.
- (3) The data for 1:2 salts with bivalent cations and monovalent anions (CaCl₂, MgCl₂, ZnBr₂, SrCl₂, ZnCl₂, and BaCl₂) have a large range in the values of the dissociation constants from 0.8 for ZnBr₂ to 3.1 for CaCl₂. If we exclude ZnBr₂ and ZnCl₂ from the analysis due to the limited number of experimental data points to which the polynomials were fitted, this range becomes 2–3.1.
- (4) FeCl₃ and Na₃PO₄—the only salts with trivalent ions in the present study—have dissociation constants of about 3.5.

We were not able to find any other consistent features in the results when we looked for patterns in the variation of the dissociation constants with the ion size, hydration number, or overall ionic strength of the solution. Tabulating and analyzing these parameters for more

compounds (e.g., organic salts) while also including other types of experimental data might provide insight in the future.

B. Predictions using the mole-fraction-based new MSOVE

In this section, we compare the predictions of the mole-fraction-based new MSOVE to experimental data from the literature^{35–45} (total 371 data points) for 11 different ternary systems. The studied solutions are mostly mixtures of chloride salts, in which case the anion is common between the two salts, except for NaBr + KBr and NaCl + NaNO₃ systems, which share a bromide anion and a sodium cation, respectively. We choose to present the results as the osmolality of the solvent by converting the reported FPD data. The data and results in terms of the root-mean-square error (RMSE) are summarized in Table III. RMSEs were calculated using the following formula:

$$\text{RMSE} = \sqrt{\frac{\sum_{i=1}^n (y_i - \bar{y}_i)^2}{n}}. \quad (18)$$

RMSEs were calculated for each subsystem separately as well as for all data points (all-system RMSE, $n = 371$), which is shown at the end of Table III. The data sources are indicated in the second column of Table III with the number of data points from each source shown in the third column. In all cases, there are one or more isopleths, meaning the dataset can be connected by a common feature, depending on the original authors' choice. For example, nine data points from Vilcu and Stanciu⁴¹ for NaBr + KBr are all equimolar mixtures ($m_{\text{NaBr}} = m_{\text{KBr}}$), while 62 data points measured by Hall *et al.*⁴⁵ for NaCl + KCl can be combined into four isopleths, each at a certain constant value of the weight ratio of the salts. The number of isopleths for each dataset and the connecting feature of each isopleth are given in the fourth and fifth columns of Table III, respectively. Additionally, across all data sources, different units of concentration are used, which are shown in the sixth column of Table III. The conversion of these units to molality is discussed in the supplementary material. The reported FPD values were converted to osmolality using Eq. (2). As mentioned before, the resulting numbers are referred to as experimental data points.

TABLE III. Summary of ternary experimental data from the literature and RMSEs for each subsystem of prediction of the mole-fraction-based new MSOVE. The all-system RMSE was calculated by considering all data points as one system (total 371 data points).

| System | Data source | Number of data points | Number of isopleths | Connecting feature | Original units | RMSE [osmoles/kg (°C)] |
|--------------------------|---|-----------------------|---------------------|--|--|------------------------|
| NaBr + KBr | Vilcu <i>et al.</i> ⁴¹ | 9 | 1 | Equimolality | FPD vs molality | 0.018 (0.034) |
| LiCl + NaCl | Gibbard <i>et al.</i> ⁴³ | 42 | 4 | Equivalent fraction wrt Li ⁺ | FPD vs equivalent concentration | 0.030 (0.056) |
| | Vilcu <i>et al.</i> ³⁸ | 5 | 1 | Equimolality | FPD vs molality | 0.020 (0.037) |
| NaCl + MgCl ₂ | Gibbard <i>et al.</i> ³⁶ | 23 | 3 | Equivalent fraction wrt Na ⁺ | FPD vs equivalent concentration | 0.050 (0.093) |
| | Haghighi <i>et al.</i> ³⁵ | 5 | 1 | wt. % of NaCl | FPD vs mass percent of MgCl ₂ | 0.391 (0.726) |
| | Mun <i>et al.</i> ⁴⁰ | 12 | 3 | Total molality | FPD vs molality | 0.077 (0.143) |
| NaCl + BaCl ₂ | Gibbard <i>et al.</i> ⁴⁴ | 21 | 3 | Equivalent fraction wrt Na ⁺ | FPD vs equivalent concentration | 0.018 (0.034) |
| LiCl + KCl | Vilcu <i>et al.</i> ³⁸ | 5 | 1 | Equimolality | FPD vs molality | 0.224 (0.417) |
| LiCl + CsCl | Vilcu <i>et al.</i> ³⁸ | 5 | 1 | Equimolality | FPD vs molality | 0.216 (0.402) |
| NaCl + KCl | Hall <i>et al.</i> ⁴⁵ | 62 | 4 | Weight ratio of salts | FPD vs total salinity | 0.108 (0.201) |
| | Vilcu <i>et al.</i> ^{38,41,42} | 13 | 1 | Equimolality | FPD vs molality | 0.197 (0.366) |
| | Haghighi <i>et al.</i> ³⁵ | 5 | 1 | wt. % of KCl | FPD vs mass percent of NaCl | 0.242 (0.450) |
| NaCl + CaCl ₂ | Gibbard <i>et al.</i> ⁴⁴ | 11 | 1 | Equivalent fraction wrt Na ⁺ | FPD vs equivalent concentration | 0.045 (0.084) |
| | Oakes <i>et al.</i> ³⁷ | 94 | 5 | Weight ratio of salts | FPD vs total salinity | 0.144 (0.268) |
| | Haghighi <i>et al.</i> ³⁵ | 5 | 1 | wt. % of CaCl ₂ | FPD vs mass percent of NaCl | 0.732 (1.356) |
| CaCl ₂ + KCl | Haghighi <i>et al.</i> ³⁵ | 5 | 1 | wt. % of KCl | FPD vs mass percent of CaCl ₂ | 1.224 (2.260) |
| NaCl + NaNO ₃ | Khitrova ³⁹ | 15 | 5 | wt. % of NaCl in the initial binary | FPD vs wt. % of salts | 0.437 (0.811) |
| | Khitrova ³⁹ | 22 | 5 | wt. % of NaNO ₃ in the initial binary | FPD vs wt. % of salts | 0.366 (0.680) |
| KCl + MgCl ₂ | Mun <i>et al.</i> ⁴⁰ | 12 | 3 | Total molality | FPD vs mole % | 0.211 (0.392) |
| | Total | 371 | 45 | | All-system RMSE | 0.240 (0.446) |

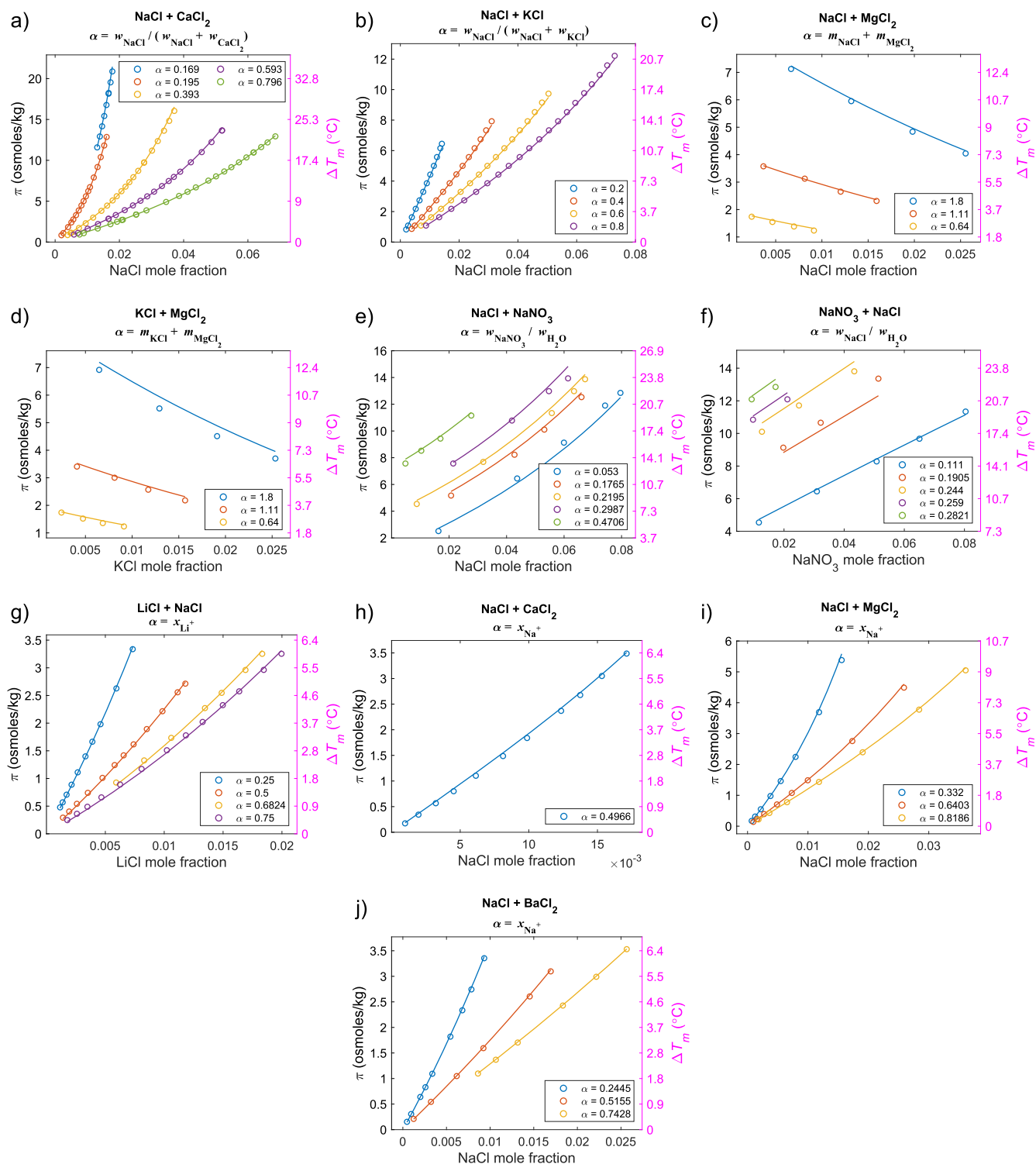


FIG. 1. Comparison of experimental data (○) with the predictions of the mole-fraction-based new MISOVE for aqueous ternary electrolyte solutions from the following sources: (a) Oakes *et al.*,³⁷ (b) Hall *et al.*,⁴⁵ (c) and (d) Mun *et al.*,⁴⁰ (e) and (f) Khitrova,³⁹ and (g)–(j) three papers by Gibbard *et al.*^{36,43,44} In the title of each panel, α indicates the connecting feature of each isopleth in that panel. Note that the π axes are linear, but the ΔT_m axes are slightly nonlinear due to the nonlinearity of Eq. (2).

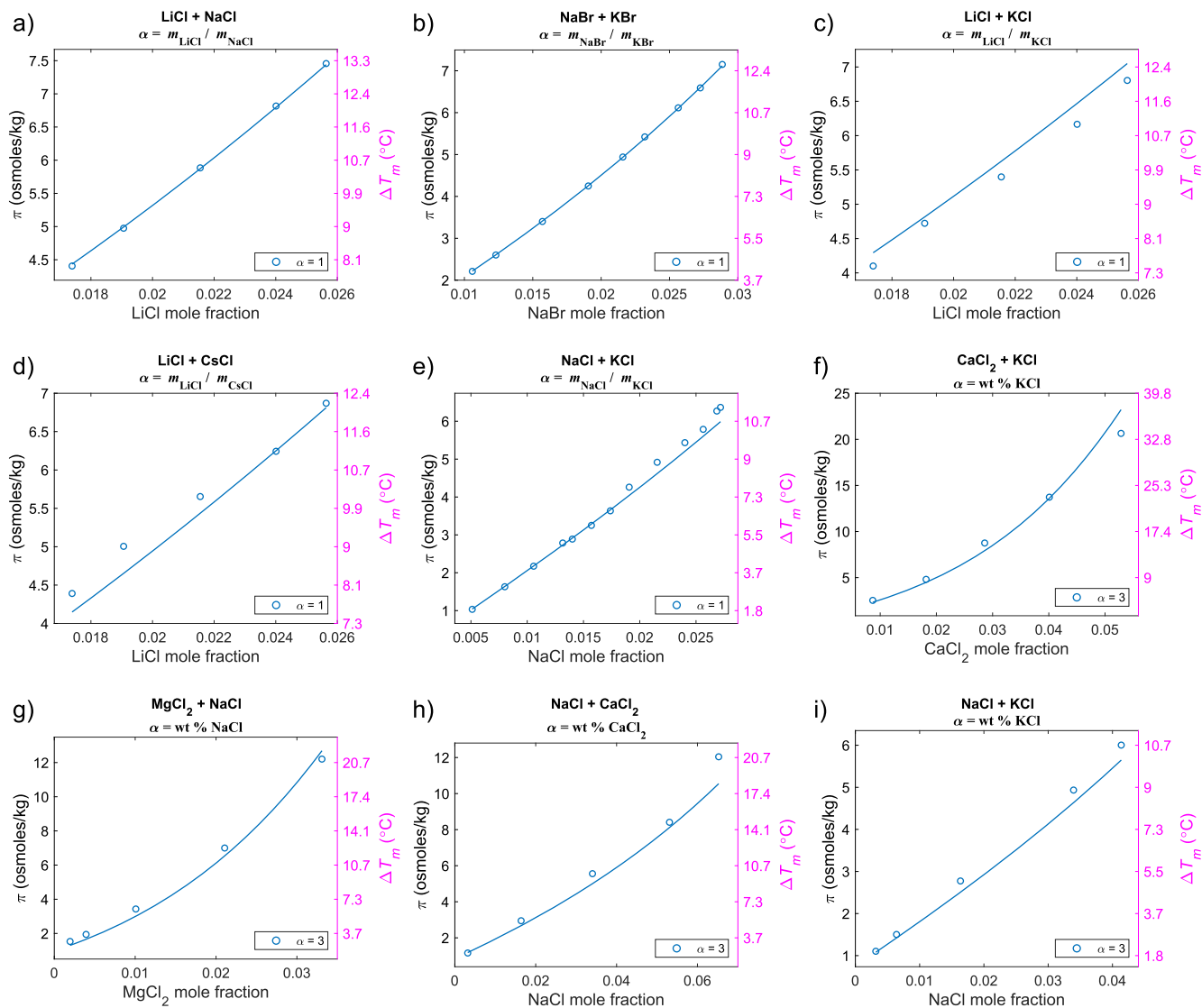


FIG. 2. Comparison of experimental data (\circ) from the given reference with the predictions of the mole-fraction-based new MSOVE for aqueous ternary electrolyte solutions from the following sources: (a)–(e) three papers by Vilcu *et al.*^{38,41,42} and (f)–(i) Haghghi *et al.*³⁵ In the title of each panel, α indicates the connecting feature of each isopleth in that panel. Note that the π axes are linear, but the ΔT_m axes are slightly nonlinear due to the nonlinearity of Eq. (2).

The fact that all data can be separated into isopleths allows us to efficiently present the goodness of the predictions graphically in 2D. The results are given in Figs. 1 and 2 for each ternary solution of each source plotted as osmolality vs mole fraction. The data are grouped so that Fig. 1 contains comparisons with data from all references listed in Table III, except for data from Haghghi *et al.*³⁵ and Vilcu *et al.*,^{38,41,42} which are given in Fig. 2. In Figs. 1 and 2, the open circles (\circ) represent the experimental data (original FPD data converted to osmolality). The solid lines of the matching color correspond to the predictions of the mole-fraction-based new MSOVE in the entire data range following the same isopleth

connecting feature, as defined in the title and in the legend of each panel.

As evident by the small RMSE values listed in Table III, as well as from Figs. 1 and 2, in most cases, the predictions of the model agree well with the experimental data. Notable exceptions with above-average RMSE values are (i) all datasets from Haghghi *et al.*³⁵ and (ii) both datasets from Khitrova³⁹ (see the supplementary material for a discussion). The all-system RMSE value of 0.24 osmoles/kg (corresponding to FPD error of 0.45 °C) was calculated by summing the squares of errors for all data points, dividing the results by the number of points (371) and taking the square root of it [see Eq. (18)]. It is small, indicating that the model

can predict the FPD of ternary electrolyte solutions well. A more detailed analysis of the errors is given in Sec. IV.

When using the MSOVE with combining rules for predictions, the apparent mismatch with experimental data or relatively large residuals can occur from three main sources: (i) inherent errors due to the simplifying assumptions of the model³¹ (e.g., the assumption of noninteracting solutes), (ii) the multisolute experimental data not being accurate, and/or (iii) the binary data used for fitting either not being accurate or not having enough data points for high fit confidence. Additionally, errors in both binary data and multisolute data can add up to result in higher apparent discrepancy, or they can cancel out to result in better apparent prediction, depending on the relative signs of the deviations. The comparison of the binary data from the sources from which the ternary data were obtained and the fitted curves that were used for predictions is given in the supplementary material.

IV. COMPARISON OF THE NEW AND ORIGINAL COMBINING RULES

In this section, we compare the prediction accuracies of the original and the new combining rules using the same dataset used in Sec. III for validation. Previously, it has been argued that the E-MSOVE can be derived both in terms of molality and mole fraction, depending on the underlying assumptions of the theory.¹⁹ Here, merely for comparison purposes, we assume that the same holds for the new MSOVE. As a result, we have four models that can be compared in terms of their predictive accuracy: (i) molality-based E-MSOVE [Eqs. (5)–(7)], (ii) mole-fraction-based E-MSOVE

[Eq. (10) with combining rules analogous to Eqs. (6) and (7)], (iii) molality-based new MSOVE [Eq. (5) with combining rules analogous to Eqs. (8) and (9)], and (iv) mole-fraction-based new MSOVE [Eqs. (8)–(10)], which is the model tested in Sec. III.

The RMSEs of all four models are presented in Fig. 3, which are grouped on a subsystem basis (see the third column of Table III). Based on this figure alone, it seems that some data are better predicted with the new MSOVE, and some data are better predicted with the E-MSOVE. However, comparing RMSEs is not enough to assess the relative performance of the models conclusively because biases may be present within each model. Furthermore, the number of experimental data points varies significantly from one subsystem to another. For example, the NaCl + KCl dataset from Hall *et al.*⁴⁵ contains 62 data points, whereas the dataset for the same system from Haghighi *et al.*³⁵ has only five data points. The systems where the RMSEs are significantly higher for the new MSOVE (both mole fraction and molality-based versions) are the CaCl₂ + KCl system from Haghighi *et al.*³⁵ with five data points and the KCl + MgCl₂ system from Mun *et al.*⁴⁰ with 12 data points.

For a more thorough comparison, we additionally performed residual analyses, the summaries of which are shown graphically in Figs. 4 and 5 for the mole-fraction-based and the molality-based models, respectively. In these figures, the top panels correspond to the new MSOVE, and the bottom panels correspond to the E-MSOVE. On the left panels, the predictions are plotted vs the measurements, and on the right panels, the residuals are plotted vs the total solute concentration. The histograms to the right of the plots show the distributions of errors, given on a log scale.

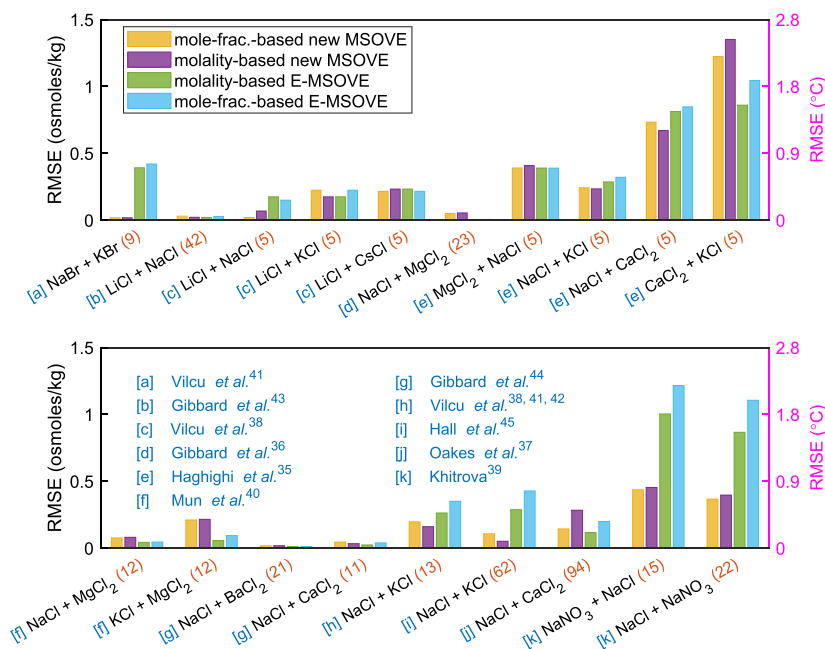


FIG. 3. RMSE values of predictions for every ternary system (separated based on the source) obtained using four versions of the MSOVE. The letters in square brackets are for the references given in blue in the legend. Note that the data from the same source are grouped so that they appear sequentially. The numbers in parentheses in red at the end of each x-axis label are the numbers of experimental data points for each system.

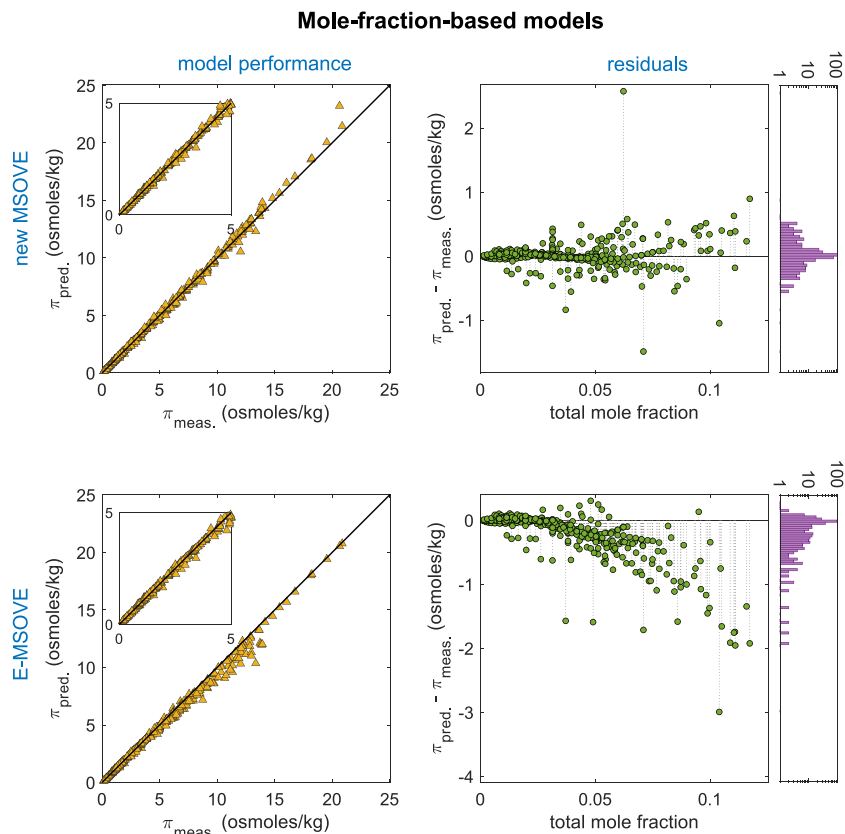


FIG. 4. Graphical representation of the performance and residuals of the mole-fraction-based models. The top panels are for the mole-fraction-based new MSOVE, and the bottom panels are for the mole-fraction-based E-MSOVE. In the left panels, the predictions are plotted against the measurements with solid black lines representing perfect prediction. In the panels on the right, the residuals are plotted against the total salt concentration for each model with a histogram to the right of the panel showing the frequency distribution of the errors. Note that the histograms are given on a log scale.

To quantitatively compare the models, we calculate all-system mean absolute error (MAE) and all-system mean bias (MB). They are defined as

$$\text{MAE} = \frac{\sum_{i=1}^n |y_i - \bar{y}_i|}{n} \quad (19)$$

and

$$\text{MB} = \frac{\sum_{i=1}^n (y_i - \bar{y}_i)}{n}, \quad (20)$$

respectively. A numerical summary of the performance of these four models in terms of RMSEs, MAEs, and MBs is presented in Table IV.

Based on Figs. 4 and 5 and Table IV, it is seen that the mole-fraction-based new MSOVE performs better in terms of RMSEs and MAEs, but more importantly, the MB is close to zero, as evident by the distribution of the errors. Both versions of the E-MSOVE have negative biases, meaning that they tend to underpredict on average. Note that although the absolute values of the MBs for the E-MSOVE predictions may still look small, they are significant because most of the experimental data points lie in the first

half of the data spread (lower concentration region), where the deviations are not as pronounced. The tendency of the E-MSOVE to underpredict is the direct result of using the geometric-average combining rule for the third-order mixed coefficients. When this combining rule is used, if one of the pure coefficients is equal to zero (e.g., when combining a second-degree fit with a third-degree fit), the entire term (which is positive since all third-order pure coefficients are positive in this study; see Tables I and II) is eliminated, whereas for the arithmetic-average combining rule this is not the case. In general, the arithmetic mean of nonnegative numbers is never smaller than their geometric mean (AM–GM inequality), so one would expect relative underprediction from the E-MSOVE even in the case of combining two third-order fits. However, the resulting discrepancy between the predictions of the models for NaCl + CaCl₂ and NaCl + MgCl₂ mixtures—the only cases where both salts have nonzero cubic coefficients—was negligible (see Fig. 3). As an example, taking the pure cubic osmotic virial coefficient values from Table I for NaCl and CaCl₂, a quick calculation shows that the arithmetic average vs geometric average combining rule only results in 0.1 osmoles/kg difference at a high salt concentration of $x_2 = x_3 = 0.05$.

Molality-based models

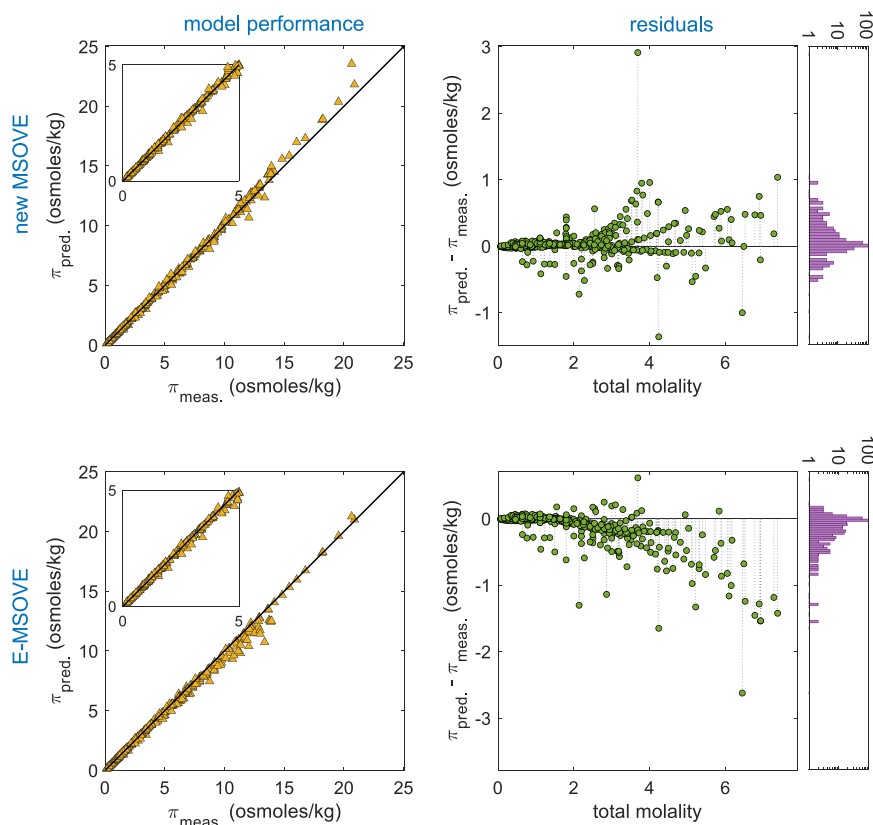


FIG. 5. Graphical representation of the performance and residuals of the molality-based models. The top panels are for the molality-based new MSOVE, and the bottom panels are for the molality-based E-MSOVE. In the left panels, the predictions are plotted against the measurements with solid black lines representing perfect prediction. In the panels on the right, the residuals are plotted against the total salt concentration for each model with a histogram to the right of the panel showing the frequency distribution of the errors. Note that the histograms are given on a log scale.

TABLE IV. Numerical summary of the performance of the models in terms of all-system RMSEs, MAEs, and MBs. All measures were calculated by considering all data points as one system (total of 371 data points).

| Model | RMSE (osmoles/kg) | MAE (osmoles/kg) | MB (osmoles/kg) |
|-------------------------------|-------------------|------------------|-----------------|
| Mole-fraction-based new MSOVE | 0.2403 | 0.1176 | 0.0145 |
| Mole-fraction-based E-MSOVE | 0.4597 | 0.2429 | -0.2204 |
| Molality-based new MSOVE | 0.2760 | 0.1336 | 0.0519 |
| Molality-based E-MSOVE | 0.3639 | 0.1831 | -0.1585 |

V. CONCLUSION

In this paper, we demonstrated that the mole-fraction-based MSOVE with arithmetic-average combining rules, recently developed by us,³¹ can accurately predict the FPD of concentrated, ternary salt solutions of water. To do this, we first empirically extended our model to account for salt dissociation by including an extra fitting parameter (the dissociation constant) for each salt in the virial expansion. Then, we fitted polynomials to single-salt–water binary

FPD data found in the literature, which are the only required inputs to the model. To determine the degree of each fitted polynomial, we proposed a unified criterion that allows the balance between the RTO-adjusted-R-squared value and the CIs of the fitted coefficients to be set with a single user-adjustable parameter. Using the proposed fitting criterion, we tabulated both the mole-fraction-based and the molality-based osmotic virial coefficients of 31 salts in water (plus the dissociation constants). Next, using the tabulated coeffi-

cients, we predicted osmolalities of 11 different aqueous solutions containing two salts. Comparison with experimental data from various sources showed that the model can predict the FPD of ternary electrolyte solutions accurately. Finally, we compared two different combining rules and concentration units and found that the mole-fraction-based model with arithmetic-average combining rules works the best for aqueous electrolytes.

We note that this article serves as a proof-of-concept since it only predicts a small set of a specific type of multisolute data from the experimental literature (i.e., FPD of water). The MSOVE with the arithmetic-average combining rules is a virial expansion for the concentration dependence of the chemical potential of the solvent; therefore, it can be used to predict a plethora of other related thermodynamic properties of multicomponent solutions (e.g., activity, fugacity, osmotic pressure, vapor pressure, etc.) for which a lot of experimental data are available in the literature for comparison. Additionally, the model's predictive capability can be tested for more complex solutions containing many species and/or different types of species (e.g., salts and proteins in the same solution).

The main benefit of the method of combining rules is that equilibrium properties of multicomponent solutions can be predicted with a minimum number of fitting parameters obtained from binary data only. The model is simple, accurate, and computationally inexpensive. However, reliable binary data are required to determine the binary polynomials to high accuracies since the errors may propagate and result in poor predictions, which would be exacerbated with increasing number of solutes. When no or limited data are available, the binary coefficients can be alternatively calculated using a more sophisticated model or inferred from molecular dynamics simulations. These coefficients can be used in suitable combining rules to obtain the mixed coefficients. Then, the MSOVE can be constructed based on these parameters and used to make predictions.

We are not aware of any model that is as simple and is able to predict the properties of multicomponent electrolyte solutions as accurately from binary data alone. Although the MSOVE and its combining rules for nonelectrolyte solutions can be derived rigorously from the theory, its extension to electrolyte solutions is purely empirical. Consequently, the good agreement between the model predictions and the experimental measurements is somewhat surprising.

SUPPLEMENTARY MATERIAL

See the supplementary material for the discussion of binary data reported in the references used for ternary data, graphical representations of binary fits, discussion of data sources and unit conversions, estimation of uncertainties in MSOVE coefficients, and numerical values of constants used in calculations.

ACKNOWLEDGMENTS

This research was funded by the Natural Sciences and Engineering Research Council (NSERC) of Canada (Nos. RGPIN-2016-05502 and RGPIN-2021-02773). H.B. acknowledges funding from the Alberta Innovates Graduate Student Scholarship. J.A.W.E. holds a Canada Research Chair in Thermodynamics.

AUTHOR DECLARATIONS

Conflict of Interest

The authors have no conflicts to disclose.

Author Contributions

H.B. collected the literature data, proposed the fitting criterion, performed the research other than that done by H.S., and wrote the first draft of this paper. As part of an undergraduate project, H.S. did the unit conversions in the supplementary material for the Gibbard *et al.* data and made predictions for the Gibbard *et al.* ternary data using the molality-based E-MSOVE with a different fitting criterion. J.A.W.E. proposed the problem, wrote the background about the E-MSOVE in the introduction section, edited the revisions of this paper, and provided supervision.

Hikmat Binyaminov: Conceptualization (equal); Data curation (equal); Formal analysis (equal); Funding acquisition (equal); Investigation (equal); Methodology (equal); Software (equal); Validation (equal); Visualization (equal); Writing – original draft (equal); Writing – review & editing (equal). **Henry Sun:** Data curation (equal); Investigation (equal); Validation (equal). **Janet A. W. Elliott:** Conceptualization (equal); Formal analysis (equal); Funding acquisition (equal); Investigation (equal); Methodology (equal); Project administration (equal); Resources (equal); Supervision (equal); Validation (equal); Writing – review & editing (equal).

DATA AVAILABILITY

Data sharing is not applicable to this article as no new data were created or analyzed in this study.

REFERENCES

- ¹G. M. Marion, R. E. Farren, and A. J. Komrowski, "Alternative pathways for seawater freezing," *Cold Regions Sci. Technol.* **29**, 259–266 (1999).
- ²D. R. Jackett, T. J. McDougall, R. Feistel, D. G. Wright, and S. M. Griffies, "Algorithms for density, potential temperature, conservative temperature, and the freezing temperature of seawater," *J. Atmos. Oceanic Technol.* **23**, 1709–1728 (2006).
- ³H. R. Pruppacher and J. D. Klett, *Microphysics of Clouds and Precipitation*, 2nd ed. (Kluwer Academic Publishers, New York, 2004).
- ⁴T. Koop, B. Luo, A. Tsias, and T. Peter, "Water activity as the determinant for homogeneous ice nucleation in aqueous solutions," *Nature* **406**, 611–614 (2000).
- ⁵D. Chao, W. Zhou, F. Xie, C. Ye, H. Li, M. Jaroniec, and S.-Z. Qiao, "Roadmap for advanced aqueous batteries: From design of materials to applications," *Sci. Adv.* **6**, eaba4098 (2020).
- ⁶Y. Yamada, K. Usui, K. Sodeyama, S. Ko, Y. Tateyama, and A. Yamada, "Hydrate-melt electrolytes for high-energy-density aqueous batteries," *Nat. Energy* **1**, 16129 (2016).
- ⁷S. Huang, J. Zhu, J. Tian, and Z. Niu, "Recent progress in the electrolytes of aqueous zinc-ion batteries," *Chem.–Eur. J.* **25**, 14480–14494 (2019).
- ⁸N. Yabuuchi, K. Kubota, M. Dahbi, and S. Komaba, "Research development on sodium-ion batteries," *Chem. Rev.* **114**, 11636–11682 (2014).
- ⁹J. Huang, Z. Guo, Y. Ma, D. Bin, Y. Wang, and Y. Xia, "Recent progress of rechargeable batteries using mild aqueous electrolytes," *Small Methods* **3**, 1800272 (2019).
- ¹⁰F. Beck and P. Rüetschi, "Rechargeable batteries with aqueous electrolytes," *Electrochim. Acta* **45**, 2467–2482 (2000).

- ¹¹Q. Zhang, Y. Ma, Y. Lu, L. Li, F. Wan, K. Zhang, and J. Chen, "Modulating electrolyte structure for ultralow temperature aqueous zinc batteries," *Nat. Commun.* **11**, 4463 (2020).
- ¹²Q. Nian, J. Wang, S. Liu, T. Sun, S. Zheng, Y. Zhang, Z. Tao, and J. Chen, "Aqueous batteries operated at $-50\text{ }^{\circ}\text{C}$," *Angew. Chem., Int. Ed.* **58**, 16994–16999 (2019).
- ¹³F. Mo, G. Liang, Q. Meng, Z. Liu, H. Li, J. Fan, and C. Zhi, "A flexible rechargeable aqueous zinc manganese-dioxide battery working at $-20\text{ }^{\circ}\text{C}$," *Energy Environ. Sci.* **12**, 706–715 (2019).
- ¹⁴J. M. Prausnitz, R. N. Lichtenthaler, and E. G. de Azevedo, *Molecular Thermodynamics of Fluid-Phase Equilibria*, 3rd ed. (Prentice Hall PTR, Upper Saddle River, NJ, 1999).
- ¹⁵J. R. Elliott and C. T. Lira, *Introductory Chemical Engineering Thermodynamics*, 2nd ed. (Prentice-Hall Inc, Upper Saddle River, 2012).
- ¹⁶J. A. W. Elliott, R. C. Prickett, H. Y. Elmoazzen, K. R. Porter, and L. E. McGann, "A multisolute osmotic virial equation for solutions of interest in biology," *J. Phys. Chem. B* **111**, 1775–1785 (2007).
- ¹⁷R. C. Prickett, J. A. W. Elliott, and L. E. McGann, "Application of the multisolute osmotic virial equation to solutions containing electrolytes," *J. Phys. Chem. B* **115**, 14531–14543 (2011).
- ¹⁸M. W. Zielinski, L. E. McGann, J. A. Nychka, and J. A. W. Elliott, "Comparison of non-ideal solution theories for multi-solute solutions in cryobiology and tabulation of required coefficients," *Cryobiology* **69**, 305–317 (2014).
- ¹⁹M. W. Zielinski, L. E. McGann, J. A. Nychka, and J. A. W. Elliott, "Nonideal solute chemical potential equation and the validity of the grouped solute approach for intracellular solution thermodynamics," *J. Phys. Chem. B* **121**, 10443–10456 (2017).
- ²⁰W. G. McMillan and J. E. Mayer, "The statistical thermodynamics of multicomponent systems," *J. Chem. Phys.* **13**, 276–305 (1945).
- ²¹T. L. Hill, "Theory of solutions," *J. Chem. Phys.* **26**, 955–956 (1957).
- ²²T. L. Hill, "Theory of solutions. II. Osmotic pressure virial expansion and light scattering in two component solutions," *J. Chem. Phys.* **30**, 93–97 (1959).
- ²³M. W. Zielinski, L. E. McGann, J. A. Nychka, and J. A. W. Elliott, "Comment on 'Determination of the quaternary phase diagram of the water–ethylene glycol–sucrose–NaCl system and a comparison between two theoretical methods for synthetic phase diagrams' Cryobiology 61 (2010) 52–57," *Cryobiology* **70**, 287–292 (2015).
- ²⁴L. U. Ross-Rodriguez, J. A. W. Elliott, and L. E. McGann, "Non-ideal solution thermodynamics of cytoplasm," *Biopreserv. Biobanking* **10**, 462–471 (2012).
- ²⁵R. C. Prickett, J. A. W. Elliott, S. Hakda, and L. E. McGann, "A non-ideal replacement for the Boyle van't Hoff equation," *Cryobiology* **57**, 130–136 (2008).
- ²⁶M. W. Zielinski, L. E. McGann, J. A. Nychka, and J. A. W. Elliott, "Measurement of grouped intracellular solute osmotic virial coefficients," *Cryobiology* **97**, 198–216 (2020).
- ²⁷L. A. Gabler Pizarro, L. E. McGann, and J. A. W. Elliott, "Permeability and osmotic parameters of human umbilical vein endothelial cells and H9C2 cells under non-ideal thermodynamic assumptions: A novel iterative fitting method," *J. Phys. Chem. B* **125**, 12934–12946 (2021).
- ²⁸L. Zargarzadeh and J. A. W. Elliott, "Comparison of the osmotic virial equation with the Margules activity model for solid–liquid equilibrium," *J. Phys. Chem. B* **123**, 1099–1107 (2019).
- ²⁹H. Y. Elmoazzen, J. A. W. Elliott, and L. E. McGann, "Osmotic transport across cell membranes in nondilute solutions: A new nondilute solute transport equation," *Biophys. J.* **96**, 2559–2571 (2009).
- ³⁰F. Liu, H. J. Chung, and J. A. W. Elliott, "Freezing of aqueous electrolytes in zinc–air batteries: Effect of composition and nanoscale confinement," *ACS Appl. Energy Mater.* **1**, 1489–1495 (2018).
- ³¹H. Binyaminov and J. A. W. Elliott, "Multicomponent solutions: Combining rules for multisolute osmotic virial coefficients," *J. Chem. Phys.* **159**, 164116 (2023).
- ³²L. D. Landau and E. M. Lifshitz, *Course of Theoretical Physics: Vol. 5: Statistical Physics* (Pergamon Press, Oxford, UK, 1980).
- ³³J. A. W. Elliott, "Gibbsian surface thermodynamics," *J. Phys. Chem. B* **124**, 10859–10878 (2020).
- ³⁴"Concentrative properties of aqueous solutions: Density, refractive index, freezing point depression, and viscosity," in *CRC Handbook of Chemistry and Physics*, 100th ed., edited by M. W. Rumble (CRC Press/Taylor & Francis, Boca Raton, FL, 2019).
- ³⁵H. Haghighi, A. Chapoy, and B. Tohidi, "Freezing point depression of electrolyte solutions: Experimental measurements and modeling using the cubic-plus-association equation of state," *Ind. Eng. Chem. Res.* **47**, 3983–3989 (2008).
- ³⁶H. F. Gibbard and A. F. Gossmann, "Freezing points of electrolyte mixtures. I. Mixtures of sodium chloride and magnesium chloride in water," *J. Solution Chem.* **3**, 385–393 (1974).
- ³⁷C. S. Oakes, R. J. Bodnar, and J. M. Simonson, "The system NaCl–CaCl₂–H₂O: I. The ice liquidus at 1 atm total pressure," *Geochim. Cosmochim. Acta* **54**, 603–610 (1990).
- ³⁸R. Vilcu, F. Irinei, and V. Isverceanu, "Thermodynamics of multicomponent electrolyte solution. IV: Individual activities in electrolyte solutions," *Bull. Soc. Chim. Belg.* **93**, 261 (1984).
- ³⁹N. N. Khitrova, "Polytherms of the ternary system NaNO₃–NaCl–H₂O," *Zh. Prikl. Khim.* **27**, 1281–1289 (1954).
- ⁴⁰A. N. Mun and R. S. Darer, "Cryoscopy of aqueous salt solutions. II. System NaCl–MgCl₂–H₂O and KCl–MgCl₂–H₂O," *Zh. Neorg. Khim.* **2**, 1658–1661 (1957).
- ⁴¹R. Vilcu and F. Stanciu, "Thermodynamic properties of aqueous electrolyte solutions II: Differential cryoscopy of sodium chloride–potassium chloride and potassium bromide–sodium bromide systems," *Rev. Roum. Chim.* **13**, 253 (1968).
- ⁴²R. Vilcu and F. Stanciu, "Differential cryoscopy in ternary system," *Rev. Roum. Chim.* **10**, 499 (1965).
- ⁴³H. F. Gibbard and A. Fawaz, "Freezing points and related properties of electrolyte solutions. II. Mixtures of lithium chloride and sodium chloride in water," *J. Solution Chem.* **3**, 745–755 (1974).
- ⁴⁴H. F. Gibbard and S. L. Fong, "Freezing points and related properties of electrolyte solutions. III. The systems NaCl–CaCl₂–H₂O and NaCl–BaCl₂–H₂O," *J. Solution Chem.* **4**, 863–872 (1975).
- ⁴⁵D. L. Hall, S. M. Sterner, and R. J. Bodnar, "Freezing point depression of NaCl–KCl–H₂O solutions," *Econ. Geol.* **83**, 197–202 (1988).

Supplementary Material for

“Predicting freezing points of ternary salt solutions with the multisolute osmotic virial equation”

Hikmat Binyaminov, Henry Sun, Janet A. W. Elliott*

Department of Chemical and Materials Engineering, University of Alberta, Edmonton, AB,
Canada, T6G 1H9

* Corresponding author: janet.elliott@ualberta.ca

This PDF file includes:

- A. Discussion of binary data reported in the references used for ternary data
- B. Graphical representations of binary fits
- C. Data sources and unit conversions
- D. Estimation of uncertainties in MSOVE coefficients
- E. Numerical values of constants

A. Discussion of binary data reported in the references used for ternary data

In Figure S1, we plot some of the binary fits and compare them with the binary data found in the sources that were used to collect the ternary solution data. Note that none of the data points shown in Figure S1 were included in the binary data used for fitting in this work. The original binary data used to generate the fit polynomials, hence, used in predictions in the RESULTS section, are from Gibbard and Gossmann^{S1} for MgCl₂, from Oakes *et al.*^{S2} for CaCl₂, and from the CRC^{S3} for the rest. The ZnBr₂ and ZnCl₂ binary data from Haghghi *et al.*^{S4} are not required for predictions because there are no ternary solution data involving these salts. We focus on the fits that were used for the prediction of ternary data reported by Haghghi *et al.*^{S4} and Khitrova,^{S5} where the predictions have relatively high, above average RMSE values (see Table 3 and Figure 6). When the fitted curves (Figure S1, panels b, c, and d) are compared the reported binary data, we notice relatively large deviations for the mentioned references. Therefore, at least some of the error in the predictions for these data sets can be attributed to the systematic mismatch of the experimental data used for binary fitting and the ternary solution data from these references. Since there were not enough binary data points in most of the ternary solution references to obtain a high-confidence fit and make predictions based on that fit, a direct comparison was not possible.

Furthermore, in Figure S1a, we show the fitted curve and its extrapolation for KCl. Since some ternary data extended beyond the data limit of the binary fit, the extrapolation region was used in these cases to make the predictions. It is clear from the plot that the binary data from Vilcu *et al.*^{S6} and from Hall *et al.*^{S7} deviate significantly from the extrapolated curve. However, it is not possible to state with confidence which is closer to the true osmolality curve. When we included the binary data points from these references for KCl fitting, the

polynomial changed from linear to quadratic, and the prediction results were not better on average, so we decided not to include these points for fitting. The highest RMSE value (1.22 osmoles/kg) for the prediction of the model is for the CaCl₂ + KCl system data from Haghghi *et al.*^{S4}. Although the reported binary data for CaCl₂ from this reference were poorly described with the binary curve (Figure S1, panel c), there were no KCl binary data for comparison. Nevertheless, it seems reasonable to assume that the prediction errors for ternary solutions that contain KCl can be, at least partially, attributed to the systematic mismatch between the results of the binary data source used for fitting (with its extrapolation) and the results of the ternary data source.

One possible reason for the mismatch is the accuracy of the experimental methods and their various biases. Additionally, the measurement accuracies are important, although, they were not always reported (see the discussion of the data sources in section S3) and even when they were reported, some are questionable. For example, Vilcu *et al.*^{S6,S8,S9} reported a temperature measurement accuracy of ± 0.0002 °C for all their works. However, Gibbard and Grossmann^{S1} found as high as 0.5 °C discrepancy when comparing their data to the Vilcu *et al.*^{S6} data, especially at molalities higher than 1.6 m. This is an indication of either different biases of two experimental methods and/or inaccurate measurements.

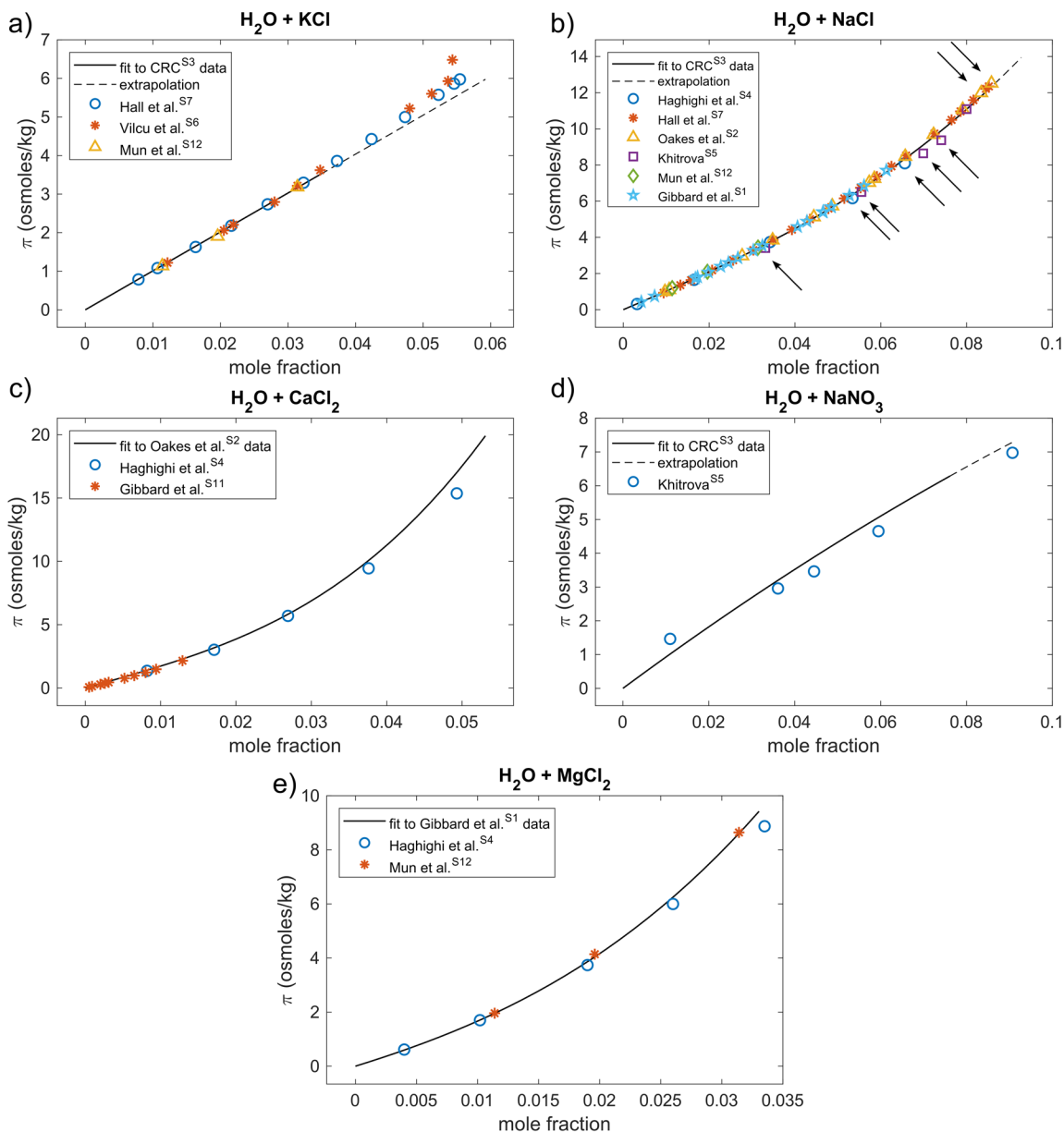


Figure S1. Comparison of some of the mole-fraction-based binary fits (black lines), used in this work to make predictions, with reported binary data from the sources from which the ternary data were obtained. Dashed lines represent extrapolation of the fitted curves. None of these data points were used for fitting in this work. In particular, note that the binary data points from Haghghi et al.^{S4} and Khitrova^{S5} are poorly described by the curves resulting from fitting to other data or their extrapolations (panels b, c, and d). Additionally, note the discrepancy between the experimental data available and the extrapolated polynomial for KCl which was used for the high-concentration prediction region (panel a). Because of the high number of data points in the NaCl plot (panel b), black arrows are used to indicate the points that have the highest deviation from the curve.

B: Graphical representations of binary fits

Visual representations of the binary data fits are given in Figure S2 (mole-fraction-based fits) and Figure S3 (molality-based fits). Binary fits were performed using multiple linear regression through the origin as described in the main text. The combined criterion described in the main text was used to determine the degree of the polynomials. The data are from Gibbard and Gossman^{S1} for MgCl₂, Oakes *et al.*^{S2} for CaCl₂, Haghghi *et al.*^{S4} for ZnBr₂ and ZnCl₂, and from the CRC^{S3} for the rest. See the main text for more details.

Mole-fraction-based fits

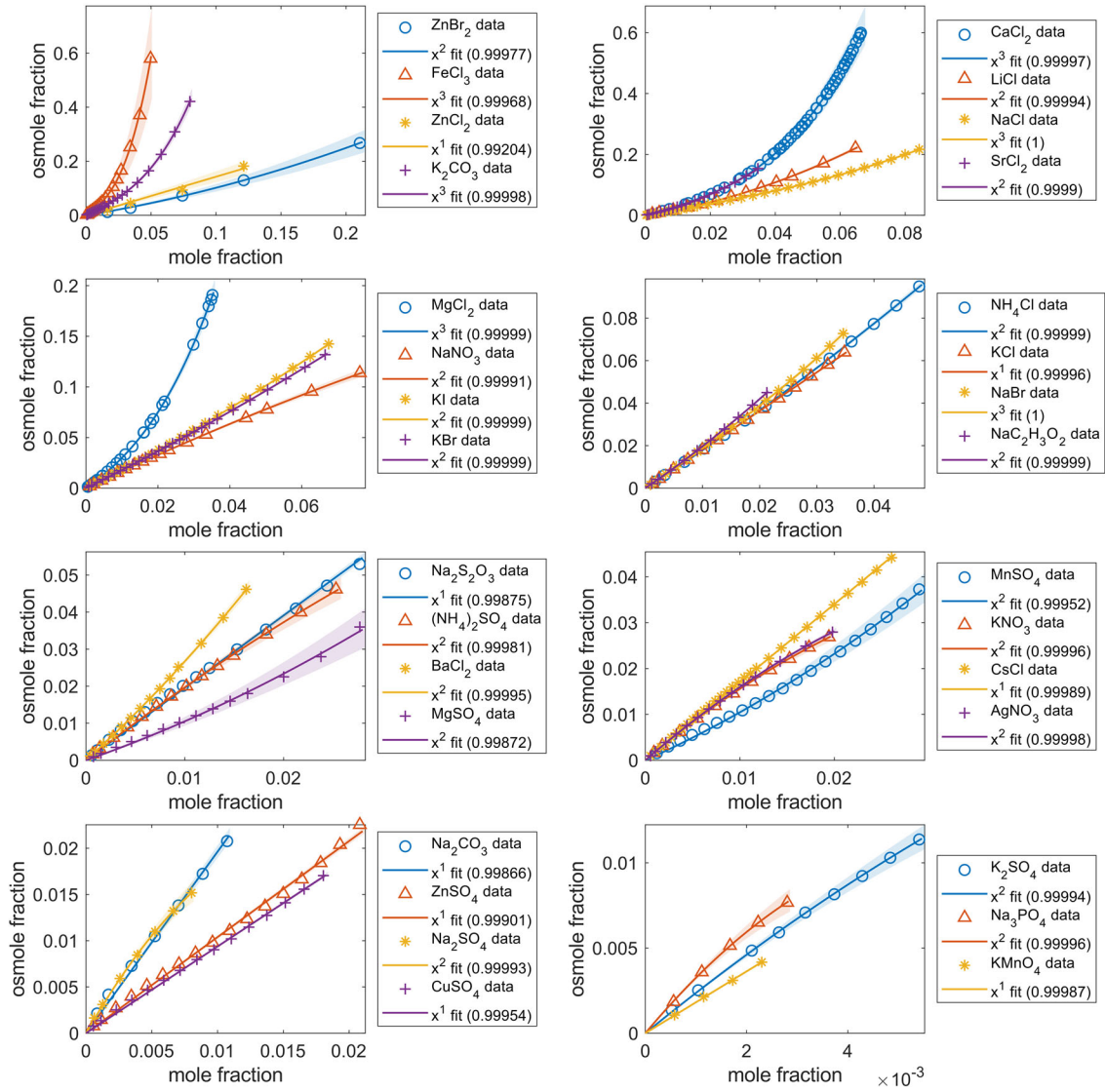


Figure S2. Mole-fraction-based fits to binary solution data plotted as osmole fraction versus mole fraction. Markers indicate the experimental data points, and solid lines of the same color indicate the best fit based on the mixed criterion described in the main text. The shaded region of the same color indicates the area where all coefficients are within their 95% CIs. The polynomial degree of each fit is given in the legend with the $R^2_{RTO,adj}$ values in parentheses.

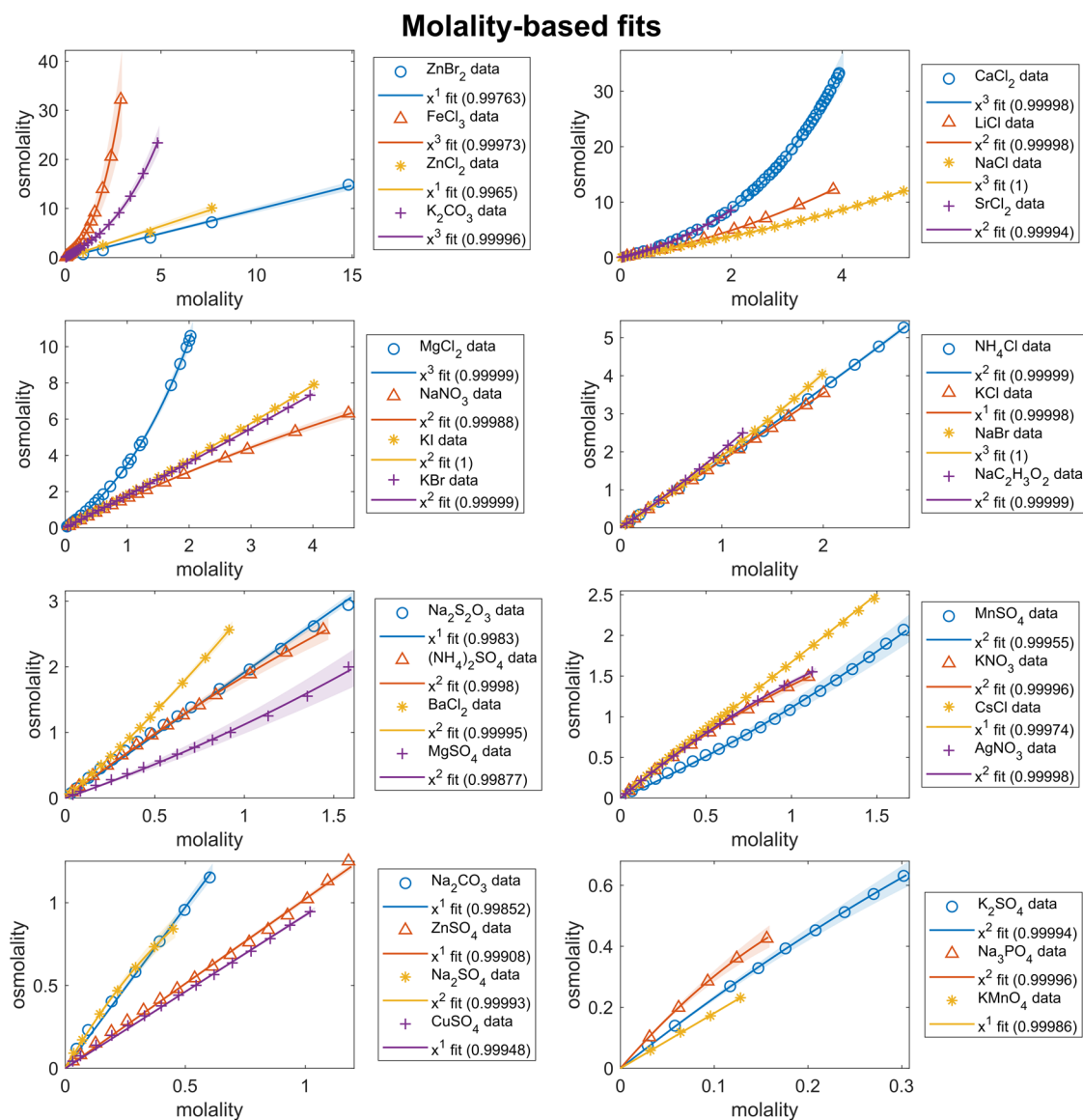


Figure S3. Molality-based fits to binary solution data plotted as osmolality versus molality. Markers indicate the experimental data points, and solid lines of the same color indicate the best fit based on the mixed criterion described in the main text. The shaded region of the same color indicates the area where all coefficients are within their 95% CIs. The polynomial degree of each fit is given in the legend with the $R^2_{RTO,adj}$ values in parentheses. The units of osmolality are osmoles/kg, and the units of molality are (moles of solute)/(kg of solvent) on these plots.

C: Data sources and unit conversions

Data for ternary solutions were obtained from multiple sources. Because of the different concentration units used, summaries for data sets from each source and the appropriate unit

conversions are given separately below. Works from the same author(s) are grouped together.

Gibbard et al.

In a series of three papers,^{S1,S15,S16} *Gibbard et al.* reported freezing point depression measurements for aqueous mixtures of: i) NaCl + MgCl₂,^{S1} ii) LiCl + NaCl,^{S10} and iii) NaCl + CaCl₂ and NaCl + BaCl₂.^{S11} In all three works, the reported accuracies were ± 0.001 °C for temperature measurements and $\pm 0.1\%$ for molality measurements.

In all three works, units of “equivalent concentration”, m' , and “equivalent fraction”, x'_i , were used. These units are represented as

$$m' = \frac{1}{2} \sum_{i=1}^{\# \text{ ion types}} m_i z_i \quad (\text{S1})$$

$$x'_i = \frac{m_i z_i}{m'} \quad (\text{S2})$$

where z_i is the charge of the ion species labeled with i and m_i is molality. For NaCl and LiCl, equation (S1) becomes (in the following equations, \times is used as a multiplication symbol in some places for clarity):

$$m' = \frac{1}{2} \sum m_i z_i = \frac{1}{2} [(m_i \times 1) + (m_i \times 1)] = m_i \quad (\text{S3})$$

That is, for 1:1 salts, the equivalent concentration equals molality. However, for 1:2 salts (MgCl₂, BaCl₂, CaCl₂), the following is obtained:

$$\begin{aligned}
m' &= \frac{1}{2} \sum m_i z_i = \frac{1}{2} [(m_{\text{cation}} \times 2) + (m_{\text{anion}} \times 1)] \\
&= \frac{1}{2} [(m_{\text{cation}} \times 2) + (2 \times m_{\text{cation}} \times 1)] = 2m_i
\end{aligned} \tag{S4}$$

In the case of 1:2 salt mixtures (*i.e.*, NaCl + BaCl₂, NaCl + CaCl₂, and NaCl + MgCl₂), x'_i , chosen to be the equivalent fraction with regards to the sodium ion ($x'_i = x_{\text{Na}^+}$), needs to be converted to the actual molality of both salts with the following conversion equations:

$$\begin{aligned}
m' &= \frac{1}{2} [(m_{\text{Na}^+}) \times 1 + (m_{\text{Cl}^-}) \times 1 + (m_{\text{Mg}^{2+}}) \times 2 + 2 \times (m_{\text{Cl}^-}) \\
&\quad \times 1] = m_{\text{NaCl}} + 2m_{\text{MgCl}_2}
\end{aligned} \tag{S5}$$

$$x'_i = x_{\text{Na}^+} = \frac{m_{\text{Na}^+}}{m_{\text{NaCl}} + 2m_{\text{MgCl}_2}} \tag{S6}$$

Isolating m_{NaCl} , we have

$$m_{\text{NaCl}} = \frac{2x_{\text{Na}^+}}{1 - x_{\text{Na}^+}} m_{\text{MgCl}_2} \tag{S7}$$

and substituting into m' , we get

$$m_{\text{NaCl}} = x_{\text{Na}^+} m' \tag{S8}$$

$$m_{\text{MgCl}_2} = \frac{1 - x_{\text{Na}^+}}{2} m' \tag{S9}$$

Similarly, for 1:1 salt mixtures (*i.e.*, LiCl + NaCl), using the same algebraic method, the following are obtained:

$$m_{\text{NaCl}} = (1 - x_{\text{Li}^+})m' \quad (\text{S10})$$

$$m_{\text{LiCl}} = x_{\text{Li}^+}m' \quad (\text{S11})$$

Furthermore, as noted in the main text, the binary MgCl_2 data were also collected from the work of Gibbard and Gossmann^{S1} to obtain the osmotic virial coefficients because this mixture is not found in the CRC^{S3}.

Haghighi et al.

Haghighi *et al.*^{S4}, measured the freezing point depression of four aqueous ternary mixtures: $\text{NaCl} + \text{KCl}$, $\text{NaCl} + \text{CaCl}_2$, $\text{KCl} + \text{CaCl}_2$, $\text{NaCl} + \text{MgCl}_2$. The reported temperature measurement accuracy is ± 0.1 °C. Additionally, the reported binary data for ZnCl_2 and ZnBr_2 from Haghighi *et al.*^{S4} were used to obtain the osmotic virial coefficients because these salts are not found in the CRC.^{S3} NaCl , CaCl_2 , MgCl_2 single-solute data were only used in the prediction plots for comparison. All four ternary data sets and all data points in every set were included for prediction accuracy evaluation. Haghighi *et al.*^{S4} reported their measurements as mass percent in the solution, and the isopleths are the constant-mass-percent curves of the second salt (see the ordering of the salts above). The formulae below were used to convert the weight percentages to molalities:

$$m_2 = \frac{w_2}{M_2(100 - w_2 - w_3)} \quad (\text{S12})$$

$$m_3 = \frac{w_3}{M_3(100 - w_2 - w_3)} \quad (\text{S13})$$

where m_2 and m_3 are the molalities, M_2 and M_3 are the molar masses, and w_2 and w_3 are the weight percentages of solutes 2 and 3, respectively, in the solution (subscript “1” is reserved for the solvent). Note that $w_3 = 3\%$ is constant for all ternary data sets from this reference.

Hall et al.

Hall et al.^{S7} measured the freezing point depression of ternary aqueous solutions of NaCl + KCl, including binary limits. All data points from this study were included in this work for comparison with MSOVE predictions. The results of Hall *et al.*^{S7} were reported as freezing point depression versus weight ratio and total salinity. As reported by the authors, the measurement uncertainties of temperature and salinity are about ± 0.05 °C and $\pm 0.02\%$ (mass percent), respectively. The weight ratios and total salinities were converted to molalities using the conversion equations given below:

$$m_{\text{NaCl}} = \frac{\bar{w}s}{M_{\text{NaCl}}(100 - s)} \quad (\text{S14})$$

$$m_{\text{KCl}} = \frac{(1 - \bar{w})s}{M_{\text{KCl}}(100 - s)} \quad (\text{S15})$$

where $\bar{w} = w_{\text{NaCl}}/(w_{\text{NaCl}} + w_{\text{CaCl}_2})$ and s are the weight ratio and total salinity, respectively.

Khitrova

Khitrova^{S5} reported ternary solution data for NaNO₃ + NaCl in terms of freezing temperature of solution versus mass percent of each component in the mixture and the

initial concentration of one of the salts in mass percent. They also reported other phase-transition data for this system, which we do not use in this work. No measurement accuracies were reported. The concentration units were converted to molality using the same equations as for Haghghi *et al.*^{S4} [equations (S12) and (S13)]. All data points for freezing point depression of solution were included in this work for comparison with MSOVE predictions.

Mun et al.

The work of Mun *et al.*^{S12} contains NaCl + MgCl₂ and KCl + MgCl₂ ternary data as freezing temperature of solution versus mole percent of the salts added and total molality of solution. No measurement accuracy was reported. To convert the total molality to the molality of each salt, we multiplied the total molality by the reported mole percent of each salt. All ternary data points from this reference were included in this work for comparison with MSOVE predictions.

Oakes et al.

Oakes *et al.*^{S2} reported freezing point depression of aqueous NaCl + CaCl₂ solutions using a similar experimental method to Hall *et al.*^{S7} The accuracy of the temperature measurements was generally better than ± 0.02 °C, and the accuracy of the solution concentration measurements was similar to that of Hall *et al.*^{S7} Additionally, we used binary CaCl₂ data from this reference for fitting. Following the methodology of the authors, we excluded five data points from their results in our work. Four of these points were from the binary data for CaCl₂. The same conversion equations were used as for the data from Hall *et al.*^{S7} [equations (S14) and (S15)], where the second equation was written for CaCl₂.

Vilcu et al.

In a series of three papers by Vilcu *et al.*,^{S6,S8,S9} the authors reported freezing point depression measurements of equimolal aqueous ternary solutions of: i) NaCl + KCl;^{S8} ii) NaCl + KCl and NaBr + KBr;^{S9} and iii) LiCl + NaCl, LiCl + KCl, LiCl + CsCl, and NaCl + KCl.^{S6} Data were reported as freezing point depression versus total molality. All data points from these works were included for comparison with MSOVE predictions. Note that no measurement accuracy was reported for the determination of concentration and the reported temperature measurement accuracy was ± 0.0002 °C. However, as noted, Gibbard and Gossmann^{S1} found as high as 0.5 °C discrepancy when comparing the measurements to their data. Furthermore, when comparing these three works by Vilcu *et al.*,^{S6,S8,S9} we found inconsistencies and round-off errors in the reported data.

D: Estimation of uncertainties in MSOVE coefficients

When fitting to binary data for electrolytes, we obtained the coefficients of the polynomial (for example, for a molality-based fit; the same holds for the mole-fraction-based fits) as $k_i, k_i^2 B_i, k_i^3 C_i$, etc. To obtain the uncertainties (here, uncertainty means a 95% CI; see the main text) in the coefficients of the virial equation (i.e., B_i 's, C_i 's, etc.), the uncertainties must be appropriately propagated upon dividing by a suitable non-negative integer power of k_i . We used standard deviation-based error propagation, that is, if $z = f(u, v)$ is a function of two independent variables u and v with uncorrelated uncertainties Δu and Δv , respectively, then the uncertainty Δz of the dependent variable z can be estimated from the following formula:^{S13}

$$(\Delta z)^2 = \left(\frac{\partial z}{\partial u}\right)^2 (\Delta u)^2 + \left(\frac{\partial z}{\partial v}\right)^2 (\Delta v)^2 \quad (\text{S16})$$

Substituting $z = u/v^h$ (where h is a nonnegative integer) and simplifying, we have

$$\frac{\Delta z}{z} = \sqrt{\left(\frac{\Delta u}{u}\right)^2 + h^2 \left(\frac{\Delta v}{v}\right)^2} \quad (\text{S17})$$

E: Numerical values of constants

The numerical values of the required constants for calculations in this work are listed in Table S1.^{S14} The molar masses of the salts were used for converting from the reported concentration units to molality and mole fraction.

Table S1. The numerical values of the required constants for calculations.^{S14}

| constant | value | units |
|------------------------------------|--------------------------|---------------------|
| $M_{\text{H}_2\text{O}}$ | 18.015×10^{-3} | kg/mole |
| M_{NaCl} | 58.443×10^{-3} | kg/mole |
| M_{KCl} | 74.551×10^{-3} | kg/mole |
| M_{MgCl_2} | 95.211×10^{-3} | kg/mole |
| M_{CaCl_2} | 110.984×10^{-3} | kg/mole |
| M_{ZnCl_2} | 136.315×10^{-3} | kg/mole |
| M_{ZnBr_2} | 225.217×10^{-3} | kg/mole |
| M_{NaNO_3} | 84.995×10^{-3} | kg/mole |
| R | 8.3145 | J/(mole \times K) |
| $\Delta S_{f,1}^\circ$ (for water) | 21.9723 | J/(mole \times K) |
| T_m^0 (for water) | 273.15 | K |

REFERENCES

- ^{S1} H. F. Gibbard and A. F. Gossmann, "Freezing of electrolyte mixtures. I. Mixtures of sodium chloride and magnesium chloride in water," *J. Solution Chem.* **3**, 385–393 (1974).
- ^{S2} C. S. Oakes, R. J. Bodnar, and J.M. Simonson, "The system NaCl-CaCl₂-H₂O: I. The ice liquidus at 1 atm total pressure," *Geochim. Cosmochim. Acta* **54**, 603–610 (1990).
- ^{S3} M. W. Rumble (editor), "Concentrative Properties of Aqueous Solutions: Density, Refractive Index, Freezing Point Depression, and Viscosity" in *CRC Handb. Chem. Phys.*, 100th ed. (CRC Press/Taylor & Francis, Boca Raton, FL, 2019).
- ^{S4} H. Haghighi, A. Chapoy, and B. Tohidi, "Freezing point depression of electrolyte solutions: Experimental measurements and modeling using the cubic-plus-association equation of state," *Ind. Eng. Chem. Res.* **47**, 3983–3989 (2008).
- ^{S5} V. A. Khitrova, "Polytherms of the ternary NaNO₃-NaCl-H₂O," *Zhurnal Prikl. Khimii* **27**, 1281-1289 (1954).
- ^{S6} R. Vilcu, F. Irinei, and V. Isverceanu, "Thermodynamics of multicomponent electrolyte solution. IV: Individual activities in electrolyte solutions," *Bull. Des Soc. Chim. Belges* **93**, 261 (1984).
- ^{S7} D. L. Hall, S. Michael Sterner, and R. J. Bodnar, "Freezing point depression of NaCl-KCl-H₂O solutions," *Econ. Geol.* **83**, 197–202 (1988).
- ^{S8} R. Vilcu and F. Stanciu, "Differential cryoscopy in ternary system," *Rev. Roum. Chim.* **10**, 499 (1965).
- ^{S9} R. Vilcu and F. Stanciu, "Thermodynamic properties of aqueous electrolyte solutions II: Differential cryoscopy of sodium chloride-potassium chloride and potassium bromide-sodium bromide systems," *Rev. Roum. Chim.* **13**, 253 (1968).
- ^{S10} H. F. Gibbard and A. Fawaz, "Freezing points and related properties of electrolyte solutions. II. Mixtures of lithium chloride and sodium chloride in water," *J. Solution Chem.* **3**, 745–755 (1974).
- ^{S11} H. F. Gibbard and S. L. Fong, "Freezing points and related properties of electrolyte solutions. III. The systems NaCl-CaCl₂-H₂O and NaCl-BaCl₂-H₂O," *J. Solution Chem.* **4**, 863–872 (1975).
- ^{S12} A. N. Mun and R. S. Darer, "Cryoscopy of aqueous salt solutions II. Systems NaCl-MgCl₂-H₂O and KCl-MgCl₂-H₂O," *Zhurnal Neorg. Khimii* **2** 834-837 (1957).
- ^{S13} H. H. Ku, "Notes on the use of propagation of error formulas," *J. Res. Natl. Bur. Stand.*

Sect. C Eng. Instrum. **70C**, 263–273 (1966).

^{S14} M. Rumble (editor), “Physical constants of inorganic compounds” in *CRC Handb. Chem. Phys.*, 100th ed. (CRC Press/Taylor & Francis, Boca Raton, FL, 2019).